

A New Model for the Joint Valuation of S&P 500 and VIX Options: Specification Analysis

Peixuan Yuan*

January, 2021

Job Market Paper

Abstract

Analyzing the specifications of pricing models for the joint valuation of S&P 500 and VIX options, I find that the existing models cannot adequately represent the two options markets. I introduce a new factor that controls the higher-order moments of the risk-neutral return distribution. The model I propose significantly outperforms all other alternatives, and particularly improves on the benchmark two-variance-factor model with co-jumps by 23.66% in-sample and 31.64% out-of-sample. The performance analysis shows that the better fit results from improvements in the modeling of both S&P 500 and VIX options, highlighting the model features that are critical for reconciling the two markets.

Keywords: Option pricing, S&P 500 and VIX joint valuation, Higher-order moments, Specification analysis, Model features.

JEL classification: G12, G13.

*Rutgers Business School, Rutgers University, 100 Rockafeller Rd, Piscataway, NJ 08854. Phone: (609)997-1398.
Email: peixuan.yuan@rutgers.edu. I am deeply indebted to my advisor, Yangru Wu, for his continuous support and guidance. I also thank Azi Ben-Rephael, Alberto G. Rossi, Ren-raw Chen, Priyank Gandhi, Hao Jiang, Zhengzi (Sophia) Li, Yuzhao Zhang, Zhaodong (Ken) Zhong, and seminar participants at Rutgers Business School, Barclays Capital, FMA Doctoral Student Consortium 2020 for helpful conversations and comments. All remaining errors are my own.

1. Introduction

The VIX index provides investors with a direct measure of volatility, being derived from S&P 500 options as the square root of the risk-neutral expectation of the integrated variance for 30 calendar days into the future. Given the widely accepted importance of volatility risk, the VIX has continuously attracted the attention of both practitioners and academics since its introduction. Not surprisingly, VIX options, which enable financial market participants to directly trade on volatility, have become the second most actively traded contracts at the Chicago Board Options Exchange (CBOE).¹ By definition, VIX options are closely linked to the S&P 500 index options but can also embed a different information set.² Therefore, in order to accurately pin down the index risk-neutral distribution, it is critical to price the S&P 500 index options in conjunction with the VIX options. Yet very little research has investigated the implication of model specifications on the joint valuation framework. This paper fills that gap by analyzing various models with different features and proposing a new model that better captures the stylized facts in the two options markets. The specification analysis sheds light on the model features that are pivotal for reconciling the two markets.

Recent empirical evidence reveals that the dynamics of the S&P 500 option surface are complex, and shows that this complexity cannot be captured well by the traditional jump-diffusion model. Andersen, Fusari, and Todorov (2015) extend the two-factor jump-diffusion model by incorporating a tail factor U_t . They show that U_t can improve the fit with S&P 500 implied volatility (IV) skew. I find, however, that when VIX options are added into the estimation dataset the root-mean-square-relative errors (RMSREs) of S&P 500 options increase by at least 12.37% in-sample and 21.60% out-of-sample.³ Furthermore, the estimated trajectory of U_t is highly dependent on whether VIX

¹In 1993, the CBOE introduced the VIX index, which was initially designed to measure the market's expectation of 30-day volatility implied by at-the-money S&P 100 Index option prices. Ten years later, in 2004, it was expanded to use options based on the more popular index, the S&P 500. CBOE launched VIX futures on March 26, 2004, and then introduced European-style options on February 24, 2006. According to the CBOE website, in 2019, VIX futures had an average daily volume of 255,000 contracts and an average daily open interest of 390,000 contracts. VIX options had an average daily volume of 534,000 and an average daily open interest of 8.4 million contracts. More details are available at <http://www.cboe.com/micro/vix/pdf/VIXfactsheet2019.pdf> and <https://www.cboe.com/micro/vix/vixwhite.pdf>.

²The VIX options can contain richer information about the higher-order moments of the S&P 500 index risk-neutral distribution. Bardgett, Gourier, and Leippold (2019) find that the S&P 500 and VIX derivatives markets contain conflicting information on the variance, especially during market distress.

³These findings are consistent with those in Bardgett et al. (2019). Because I estimate models using a longer sample period, however, I find a much larger effect of including VIX options on the fit with S&P 500 options. Furthermore, I assign equal weight to both markets during the estimation, which results in much lower pricing errors of VIX options

options are included. These findings imply that VIX options indeed contain information that conflicts with the information embedded in S&P 500 options, and that, importantly, the model cannot fully represent both options markets. A more advanced model for the joint valuation of S&P 500 and VIX options is therefore warranted.

My main contribution to the joint pricing literature is to introduce a new factor, Z_t , which partially drives the dynamics of volatility of volatility and the intensity of volatility jumps. Specifically, the new model incorporates two diffusion parts ($B_{1,t}$ and $B_{2,t}$) in the volatility process V_t . The (local) volatility of $B_{1,t}$ is driven by V_t , whereas the (local) volatility of $B_{2,t}$ is controlled by Z_t . Including Z_t can significantly increase the model's capacity to capture the dynamics of the risk-neutral distribution of return variance while keeping the model within the affine model class.

The first benefit of incorporating Z_t is that the model can simultaneously capture the leverage effect and asymmetric volatility property, each of which are critical for pricing S&P 500 and VIX options, respectively. The leverage effect represents negative changes in returns that are strongly related to increases in volatility, and the asymmetric volatility property refers to the fact that the volatility of the VIX varies asymmetrically in response to changes in the VIX (see, e.g., Park (2016)). A successful joint pricing model should therefore accommodate both features. In particular, by allowing a negative correlation between the diffusion part in returns and $B_{1,t}$, and a positive correlation between the diffusion part in Z_t and $B_{2,t}$, my model can effectively capture both the leverage effect and asymmetric volatility property. The existing models in the literature, however, can incorporate only either one of the two features or the other, not both. The models in Andersen et al. (2015) and Bardgett et al. (2019), for example, capture the leverage effect only, whereas the model in Park (2016) accommodates asymmetric volatility only.

Importantly, factor Z_t also contributes to diffusive volatility of volatility. Although volatility and volatility of volatility are correlated, they exhibit distinct revolutions. Therefore, including Z_t can drive a wedge between their dynamics and thus improves the model fit with VIX options. Another critical feature of Z_t in my model framework is that it can potentially capture the negative correlation between S&P 500 at-the-money (ATM) IVs and VIX skew, defined as the deep out-of-the-money call IVs minus the deep OTM put IVs. The negative relationship stems from the nature of the mean-reverting property of volatilities. Specifically, market participants believe that large

than those reported in Bardgett et al. (2019).

upward movements in market volatility are less likely to happen when the volatility is already at a high level (e.g., the 2008 financial crisis). This feature, however, is widely ignored in the literature. In the most existing models, a high level of volatility always implies a high value of volatility skew.

Another essential contribution of Z_t is that it can potentially improve the performance of S&P 500 options under the joint valuation framework, although it may have little direct impact on the S&P IV surface. The indirect impact of Z_t on S&P 500 options can come from two of its attributes. First, it plays a pivotal role in pricing VIX options and, as such, frees other risk factors to better capture the features of S&P 500 options. Because of the conflicting information contained in S&P 500 and VIX options, excluding Z_t will force the dominant factors of the S&P 500 options to drive the dynamics of VIX IV surface. Second, it enables the model structure (including estimated parameters) more representative to both markets.

By extending the works of Andersen et al. (2015) and Bardgett et al. (2019), I show that risk factor U_t , which controls the jump intensity of negative jumps in returns and positive jumps in volatility, also plays a pivotal role in pricing VIX options. In particular, including U_t can improve the model fits with both S&P 500 and VIX IV skews. Importantly, U_t generates a positive relation between VIX ATM IV and skew. This pattern can be observed at the end of the sample period in this paper, during which both long-term volatility and volatility skew have continually increased. U_t , however, can directly affect the volatility process through the contemporaneous jumps (co-jumps) in returns and volatilities. As a result, co-jumps can also make a significant improvement in the pricing of S&P 500 and VIX options.

Based on the seminal paper of Duffie, Pan, and Singleton (2000) , I develop a general affine jump-diffusion pricing model for the joint valuation framework, which includes a wide range of nested models. The affine structure allows me to price S&P 500 and VIX options in a semi-closed form, which facilitates the estimation using a large dataset of options and a comparison with other alternative affine models. The full specification model, denoted 4F-ICJ, features two variance factors, co-jumps, and factors Z_t and U_t . The models are then tested on the two sets of market data covering April 4, 2007 through December 27, 2017.

Turning to the empirical results, I first find that the 4F-ICJ model significantly outperforms all other alternative models, both in- and out-of-sample. In particular, it improves the overall performance of the benchmark two-variance-factor model with co-jumps, denoted 2F-CJ, by 23.66%

in-sample and 31.64% out-of-sample. Focusing on the specific options market, I find that the 4F-ICJ model reduces the pricing errors of the 2F-CJ model by 15.07% (31.70%) in-sample and 27.25% (36.04%) out-of-sample for S&P 500 options (VIX options). Importantly, the 4F-ICJ model continues to outperform all other nested models in each options market. Furthermore, the pricing error analysis shows that the 4F-ICJ model has a minimal structure in the errors on the S&P 500 and VIX options. Specifically, the mean pricing errors of the 4F-ICJ model are close to zero and show no apparent structures along both the moneyness and maturity dimensions. To further dispel the concern that 4F-ICJ is richly parameterized, which may result in overfitting, I compare the capacity of the models to fit the option characteristics. The result shows that the 4F-ICJ model's implied characteristics closely track those of their counterparts observed in the markets. In particular, the 4F-ICJ model provides the lowest-fitting errors of option characteristics, both in- and out-of-sample. The superior performance of the 4F-ICJ model is therefore not due to its rich specification or in-sample overfitting.

I next look at the models that either exclude U_t , denoted 3FZ-ICJ, or exclude Z_t , denoted 3FU-CJ, from the 4F-ICJ model. Compared with the 4F-ICJ model, these two models exhibit relatively less stable pricing performance, both in- and out-of-sample. However, they both also significantly outperform the benchmark for pricing S&P 500 and VIX options during the full sample period, which implies that they are not overfitted. Inspection of the pricing errors of VIX options reveals that the 3FZ-ICJ model performs better than the 3FU-CJ model during the in-sample period but produces a higher out-of-sample error. I find that Z_t is relatively more important for capturing VIX skew during market turmoil, which happens more frequently during the in-sample period. Interestingly, however, U_t is critical for capturing VIX skew during times of market tranquility, which is the typical feature during the out-of-sample period.⁴ In particular, both long-term VIX ATM IV and skew are continually increasing at the end of the out-of-sample. Both Z_t and U_t are therefore indispensable in the joint pricing framework, which further supports the superiority of the 4F-ICJ model.

Finally, I also find that the co-jumps are critical for jointly pricing S&P 500 and VIX options because excluding the co-jumps from the 4F-ICJ model, which leads to the 4F-IJ model, can significantly deteriorate the performance. The 4F-IJ model performs worse than the 4F-ICJ model

⁴Bardgett et al. (2019) also find that factor U_t reaches its lowest level during the 2008 financial crisis.

for pricing S&P 500 options in both in- and out-of-sample periods. Interestingly, the 4F-IJ model performs as well as the 4F-ICJ model for pricing in-sample VIX options but significantly underperforms during the out-of-sample period. This finding also proves the importance of U_t which can directly affect the risk-neutral distribution of return variance through co-jumps. Importantly, when U_t is excluded, the 4F-IJ model can easily result in an overfitted estimation of VIX options.

To provide more insight into the 4F-ICJ model, I extensively investigate its properties by conducting several simulations. I show the distinct roles of the factors Z_t and U_t in capturing S&P 500 and VIX IV characteristics. I construct simulated IV smiles of the two options markets by changing the levels of different factors with estimated model parameters. The empirical analysis yields the following key results. First, both factors have distinct yet complementary roles in the joint valuation framework. Second, both S&P 500 and VIX options contribute to pinning down the dynamics of U_t . Third, factor Z_t can only be identified by including VIX options in the model estimation. The findings further support the importance of the joint valuation model, and they also imply that the VIX options contain valuable information on the dynamic of index risk-neutral distribution that is not spanned by S&P 500 options. Finally, by performing a Monte Carlo simulation study, I illustrate how the 4F-ICJ model captures the well-documented asymmetric volatility property.

This paper is related to the literature on consistent VIX option pricing models that specify the dynamics of equity index returns (e.g., Sepp (2008), Lin and Chang (2010), Chung, Tsai, Wang, and Weng (2011), Cont and Kokholm (2013)). These studies attempt to reproduce the IV smiles of S&P 500 and VIX options simultaneously. I build on this literature by proposing a new family of affine jump-diffusion frameworks that nests the commonly studied models. I also extend the previous studies by estimating the time-consistent models on a large option panel data set that spans ten years and includes all qualified contracts in both options markets. In contrast with mine, most of the previous studies restrict their analysis to a static one-day estimation and a limited sample, losing a large part of the information and resulting in significant variations in estimated parameters over time.

Bardgett et al. (2019) apply a model that is similar to the 3FU-CJ model in this paper to infer volatility dynamics and risk premia from the S&P 500 and VIX markets. They find that VIX markets contain information that is not spanned by S&P 500 options, since including VIX

option prices in the model estimation allows for better identification of the parameters controlling the dynamics of return variance. I confirm their findings, however, by showing that including VIX options in the estimation can significantly deteriorate the performance of their model for pricing S&P 500 options. This finding also implies that their model cannot adequately represent both options markets. Furthermore, their model neither includes a stochastic volatility-of-volatility factor nor captures the asymmetric volatility property. In addition to proposing a new model, this paper also focuses on the model specification analysis of both S&P 500 and VIX options and uncovers the model features that are required to reconcile the conflicting information embedded in the two markets.

Branger, Kraftschik, and Völkert (2016) studies a model that also incorporates a volatility-of-volatility factor. However, their model can capture neither the leverage effect nor the asymmetric volatility property that are critical features in the S&P 500 and VIX markets, respectively. Furthermore, they estimate models on VIX options only and, as such, largely ignore the information embedded in S&P 500 options. In particular, by incorporating the information from S&P 500 options, I find both co-jumps and U_t are crucial for pricing VIX options.

My work is also related to the literature on the reduced VIX option pricing models which directly assume the dynamics of the volatility index, e.g., Grünbichler and Longstaff (1996), Mencía and Sentana (2013), Park (2016), and among others. By definition, VIX options, however, are closely related to S&P 500 options. This paper aims to connect the two markets by extensively investigating the model specifications under a joint valuation framework. Importantly, it sheds new light on the features of the model that are critical for capturing the stylized facts of both markets over time.

Finally, this paper also enriches the literature on pricing S&P 500 index options (e.g., Bakshi, Cao, and Chen (1997), Bates (2000), Pan (2002), Eraker, Johannes, and Polson (2003), Christoffersen, Heston, and Jacobs (2009), Andersen et al. (2015)). In particular, I highlight the importance of co-jumps by jointly pricing S&P 500 and VIX options. VIX options that portray the conditional density of future VIX levels may contain much comprehensive information on the dynamics of the S&P 500 return variance. Therefore, including VIX options can better identify the parameters driving the risk-neutral conditional distributions of volatility (see, e.g., Bardgett et al. (2019)).

The rest of this paper is organized as follows. Section 2 describes the S&P 500 and VIX options data and highlights the stylized facts in each market. Section 3 lays out the pricing model

and introduces the estimation methodology. Section 4 discusses the parameter estimates. Section 5 analyzes the pricing performance across the different model specifications. Section 6 investigates the properties of the pricing model. Section 7 concludes. The Appendix contains technical derivations.

2. Data and Preliminary Analysis

2.1. Data description

I use European-style S&P 500 equity-index (SPX) and VIX options traded at the Chicago Board Options Exchange (CBOE). The option quotes are obtained from OptionMetrics. The VIX options were introduced in 2006. Because the trading of VIX options was inactive in the first year after it was introduced, the sample spans the period from April 2, 2007 to December 29, 2017. Following earlier empirical work (e.g., Christoffersen et al. (2009); Andersen et al. (2015)), I sample the options data every Wednesday to avoid weekday effects, resulting in a total of 557 weeks. The sample is further divided into an in-sample period covering April 4, 2007 to April 1, 2015, and an out-of-sample period April 8, 2015 to December 27, 2017.

I restrict the analysis to VIX options with days to maturity ranging from 7 to 160 days and S&P 500 options with days to maturity ranging from 7 days to a year. To address illiquidity and microstructure concerns, I apply various filters that are commonly used by previous parametric studies (see., e.g., Bakshi et al. (1997)). Specifically, I eliminate option quotes that do not satisfy standard no-arbitrage conditions and report zero trading volume on a given date. I further delete options with negative bid-ask spreads and options for which the implied volatility cannot be calculated. Moreover, out-of-the-money (OTM) options tend to be more liquid than in-the-money options. For this reason, I only work with liquid OTM call and put options. These adjustments leave a total of 237,075 S&P 500 options and 32,203 VIX options, with a daily average of 426 S&P 500 options and 58 VIX options.

VIX option prices do not satisfy no-arbitrage relations with respect to the VIX index, but do satisfy them with respect to the VIX futures value. The underlying of VIX options is therefore the VIX futures, not the VIX itself. Following Bardgett et al. (2019), I infer from highly liquid options the VIX futures price using the at-the-money (ATM) put-call parity.

2.2. Summary statistics

I denote European-style OTM option prices for the asset X (e.g., SPX or VIX) at time t by $O_X(t, T, k)$. I measure moneyness by $k = K/F(t, T)$, where $F(t, T)$ is the future price with time to maturity T at t , and K denotes the strike price.⁵ I also define DTM as days to maturity which measures the tenor of the option.

[Insert Tables 1 and 2 near here]

Table 1 describes the S&P 500 index options sorted by days to maturity (DTM) and moneyness (K/F). Panel C reports the average IVs for each bin. The IVs are computed using the standard Black-Scholes formula. Consistent with previous studies, I observe pronounced patterns of negative option IV skew across different DTM bins. These patterns are due to the expensiveness of OTM put options on the S&P 500. OTM put options provide investors with a hedge to downward movements in returns and, as such, attract risk-aversion investors to hold them.

Table 2 presents descriptive statistics for the VIX option quotes. In contrast to the pattern shown in Table 1, pronounced upward sloping patterns in VIX IVs are evident in Panel C across all DTM bins, with short-term options exhibiting the steepest volatility skew. Furthermore, VIX call options are more heavily traded than put options due to the leverage effect. Negative changes in market return are accompanied by increases in volatility, indicating that OTM call options on the VIX can provide disaster insurance for the overall equity market. Market participants therefore use OTM VIX call options to protect their portfolios against sharp increases in volatility and decreases in market price.

[Insert Figures 1 and 2 near here]

Panel A in Figure 1 plots the temporal variation of the number of S&P 500 options for different DTM bins. We can notice that the number of short-term contracts continuously increases since the beginning of the sample period. The options whose $DTM > 180$ days, however, keep around 40 contracts per day. Panel B in Figure 1 presents the time variation of the number of contracts for different K/F bins. The figure shows that the number of contracts for each bin has dramatically increased since 2007. Another notable feature is that the trading activities of both deep OTM

⁵For simplicity, hereinafter, I use F instead of $F(t, T)$ to present the future price with time to maturity T at t .

puts ($K/F < 0.85$) and calls ($1.03 \leq K/F$) dominate others most of the time. Interestingly, the moderate OTM options (e.g., $0.95 \leq K/F < 0.98$ and $1 \leq K/F < 1.03$) exceeded other types in 2017.

Panel C in Figure 1 shows the time variation of the term structure of S&P 500 IVs. It has several noteworthy features. First (and unsurprisingly), the overall level of the IV term structure is time-varying. The most extreme IV levels are observed in the 2008 financial crisis. Second, the slope of the IV term structure also varies significantly over time, with the short-term IV exceeding the long-term during crises. Panel D displays the temporal variation of an IV smile. A downward-sloping IV smile is observed throughout the whole sample period, where the IV of OTM put is consistently higher than that of OTM call.

Next, I explore the VIX option panel data by plotting various figures in Figure 2. Panel A plots the temporal variation of the number of VIX options for different DTM bins. One can notice that the number of contracts for each DTM bin has also dramatically increased since 2007. Furthermore, the trading of short-term contracts is relatively more active at the beginning of the sample period. However, the number of long-term options increased to a level close to that of short-term contracts at the end of the sample.⁶

Panel B further illustrates the time variation in the number of options contracts for different K/F bins. As expected, I continue to observe an upward trend in the number of contracts in all K/F bins. Importantly, the number of OTM call options significantly increased in 2017 and even dominated all other types of options that year.

Panel C plots the time variation of the term structure of VIX IV. In general, the IV term structure slopes downward. Furthermore, both the short- and long-end of IV term structure show substantial time variations, with the short end increasing dramatically during crises. Panel D shows that the IV of deep OTM call options is generally larger than that of deep OTM put options and that the IV smile changes significantly over time.

⁶Worries about long-term volatility risk, which intensified toward the end of sample period, exert a significant impact on pricing models.

2.3. The option surface characteristics

In this section, I investigate the relationships between the IV surfaces of S&P 500 and VIX options. The main interest of this paper is to analyze the capacity of the models for jointly pricing S&P 500 and VIX options. It is therefore critical to figure out the connection between these two markets.⁷

The option IV surface displays highly persistent and nonlinear dynamics that are difficult to analyze effectively. I therefore first summarize the IV surface through two of its characteristics: skew and at-the-money (ATM) IV. I measure the skew of S&P 500 (VIX) options as the IV of deep OTM puts (calls) minus the IV of deep OTM calls (puts). ATM options have moneyness, K/F , close to 1.⁸

[Insert Figures 3 and 4 near here]

Figure 3 displays the scatter plots of SPX ATM IV and the characteristics of VIX IVs. As expected, Panel A shows that there is a positive relation between SPX ATM IV and VIX ATM IV, indicating the existence of common factors that control the levels of both IV surfaces. Panel C, however, shows that this relation is quite weak for long-term IVs. Interestingly, there is a significantly negative relationship between SPX ATM IV and VIX skew for both short- and long-term IVs. This relationship stems from the nature of the mean-reverting property of volatilities. Specifically, market participants believe that large upward movements in market volatility (VIX) are less likely to happen when the VIX is already at a high level. A successful joint pricing model should therefore accommodate both of these two features simultaneously. Later in the paper I show that the new factor that I propose here can capture these patterns.

Figure 4 shows the scatter plots of SPX skew and the characteristics of VIX IVs. Panel A shows that the correlation between the SPX skew and the VIX ATM IV is significantly positive. This pattern can be partially captured by co-jumps with a time-varying jump intensity (e.g., contemporaneously negative (positive) jumps in returns (volatilities)). Specifically, a high jump intensity

⁷I restrict the analysis to the connection between the two markets. A number of articles provide detailed analyses of the characteristics of each option market (see, e.g., Bakshi et al. (1997), Christoffersen et al. (2009), Eraker et al. (2003) and Andersen et al. (2015) for S&P 500 options, and Mencía and Sentana (2013), Park (2016), Branger et al. (2016) and Bardgett et al. (2019) for VIX options).

⁸I separately analyze the characteristics of the short- and long-term IVs instead of looking at the term structure. The main reason is that the magnitude of short-term VIX IV dominates that of long-term VIX IV.

of negative jumps in returns can generate high SPX skew. Simultaneously, it can also increase the vol-of-vol and thus the VIX ATM IV through positive jumps in volatilities. Importantly, Panel B shows that a high SPX skew corresponds to a low VIX skew. This pattern, however, contrasts with the above argument because a high jump intensity in positive volatility jumps also implies a high VIX skew in the standard co-jump setting. As a result, co-jumps alone cannot capture the patterns in Panels A and B. Panels C and D show similar but weaker patterns for long-term IVs.

In summary, the S&P 500 and VIX options markets are closely related in a complicated way, and their trading activities have significantly increased since their introduction. However, they also contain different characteristics and information about their underlyings. The S&P 500 options, assuming a continuous range of traded strikes, characterize the conditional density of future S&P 500 returns. The VIX options, however, portray the conditional density of future VIX levels, and as such, contain more information on the future density of S&P 500 return variance (Bardgett et al. (2019)). Therefore, in order to fully characterize the future density of both return and variance, the joint valuation of S&P 500 and VIX options is warranted.

3. Model and Estimation

3.1. Model specification

In this section, I investigate the parametric modeling of the S&P 500 and VIX options. Inspired by Mencía and Sentana (2013), Andersen et al. (2015) and Bardgett et al. (2019), I introduce a tractable framework for jointly pricing options in the presence of multiple stochastic risk factors and jumps. The model is novel in both the S&P 500 and the VIX options pricing literature and able to capture essential facts in the two options markets simultaneously. The model I propose also embeds most existing continuous-time models in the literature as special cases, which facilitates our efforts to investigate the importance of the model's features.

I use $(\Omega, \mathcal{F}, \{\mathcal{F}_t\}_{t \geq 0}, \mathbb{Q})$ to denote a complete stochastic basis defined on the risk-neutral measure

\mathbb{Q} , under which the model for the risk-neutral equity index dynamics is given by

$$dS_t/S_t = (r_t - q_t) dt + \sqrt{V_t} dB_t + \int_{\mathbb{R}^2} (e^x - 1) \tilde{\mu}(dx, dt), \quad (1)$$

$$\begin{aligned} dV_t &= \kappa_v (m_t - V_t) dt + \sigma_v \sqrt{V_t} dB_{1,t} + \varsigma \sqrt{Z_t} dB_{2,t}, \\ &\quad + \int_{\mathbb{R}^+} y \pi(dy, dt) - \eta_1 \int_{\mathbb{R}^2} x \cdot 1_{\{x<0\}} \mu(dx, dt), \end{aligned} \quad (2)$$

$$dm_t = \kappa_m (\theta_m - m_t) dt + \sigma_m \sqrt{m_t} dB_{m,t}, \quad (3)$$

$$dZ_t = \kappa_z (\theta_z - Z_t) dt + \sigma_z \sqrt{Z_t} dB_{z,t} - \eta_2 \int_{\mathbb{R}^2} x \cdot 1_{\{x<0\}} \mu(dx, dt), \quad (4)$$

$$dU_t = \kappa_u (\theta_u - U_t) dt + \sigma_u \sqrt{U_t} dB_{u,t}, \quad (5)$$

where $(W_t, B_{1,t}, B_{2,t}, B_{m,t}, B_{z,t}, B_{u,t})$ is a six-dimensional Brownian motion. I allow the Brownian motions W_t in Equation (1) and Brownian motions $B_{1,t}$ in Equation (2) to be correlated, $\rho_1 dt = \mathbb{E}[dW_t dB_{1,t}]$. I further allow the Brownian motions $B_{2,t}$ in Equation (2) and Brownian motions $B_{z,t}$ in Equation (4) to be correlated, $\rho_2 dt = \mathbb{E}[dB_{2,t} dB_{z,t}]$. All other Brownian motions are mutually independent. In addition, μ is an integer-valued measure counting the jumps in the price, S , and the state vector, (V, Z) . The corresponding (instantaneous) jump intensity, under the risk-neutral measure, is $dt \otimes v_{1,t}(dx)$. The difference $\tilde{\mu}(dx, dt) = \mu(dt, dx) - v_{1,t}(dx)dt$ constitutes the associated martingale jump measure. Similarly, π counts the independent jumps in V , and the corresponding jump intensity is measured by $dt \otimes v_{2,t}(dy)$. The compensators characterize the conditional jump distribution and are given by

$$\frac{v_{1,t}(dx)}{dx} = \lambda_t^+ \cdot 1_{\{x>0\}} e^{-x/\delta_1^+}/\delta_1^+ + \lambda_t^- \cdot 1_{\{x<0\}} e^{-x/\delta_1^-}/|\delta_1^-|, \quad (6)$$

$$\frac{v_{2,t}(dy)}{dy} = \xi_t \cdot 1_{\{y>0\}} e^{-y/\delta_2}/\delta_2. \quad (7)$$

Following Kou (2002), I model the price jumps as exponentially distributed. Upward jump magnitudes are assumed to follow an independent exponential distribution with a positive mean, $\delta_1^+ > 0$. Downward jump magnitudes are assumed to follow an independent exponential distribution with a negative mean, $\delta_1^- < 0$. Inspired by Park (2016), I only consider upward jumps in the Equation (7). The mean of the independent upward jumps in factor Z is $\delta_2 > 0$. Finally, the time-varying jump intensities in Equation (6) are governed by the λ_t^+ and λ_t^- coefficients and are

given by

$$\lambda_t^+ = \lambda_0^+ + \lambda_1^+ V_t + \lambda_2^+ m_t, \quad \lambda_t^- = \lambda_0^- + \lambda_1^- V_t + \lambda_2^- m_t + \lambda_2^- U_t, \quad (8)$$

and the jump intensity in Equation (7) is given by

$$\xi_t = \xi_0 + \xi_1 V_t + \xi_2 Z_t. \quad (9)$$

The model involves a broad set of parameters that can be hard to identify separately. At the estimation stage, following Andersen et al. (2015), I eliminate those that are insignificant and have no discernible impact on model fit. For identification purposes, I set θ_z and θ_u to 1.

The model possesses several distinctive features. The factor V drives both the diffusive volatility and the jump intensities. It also partially drives the volatility itself. The most distinct feature of the model is that it includes a new factor, Z . First, Z contributes to diffusive volatility of volatility if $\varsigma > 0$. Stochastic volatility of volatility is crucial for pricing VIX options (Mencía and Sentana (2013)). Incorporating Z can capture the asymmetric behavior of volatility if ρ_2 is nonzero.⁹ The nonzero ρ_2 can help induce the fatter tail of the risk-neutral distribution of volatility. Second, Z also contributes to the jump intensity of the independent jumps in V . Therefore, Z largely controls the tail behavior of the volatility. The co-jumps also occur in factor Z if η_2 is nonzero. If $\eta_2 > 0$, large negative movements in equity returns, large positive movements in volatility, and large positive movements in the volatility of volatility can occur at the same time.¹⁰ I also allow positive and negative jump intensities to have different loadings on the latent factors.

The factor m drives the stochastic level around which V reverts. It has already been shown that the m factor is needed to provide an accurate description of the volatility dynamics. Mencía and Sentana (2013) points out that m is crucial for capturing the term structure of volatility and therefore also VIX futures. Finally, the factor U affects the jump intensities of the co-jumps. It contributes only to negative jumps in equity returns and thus helps capture the stochastic skew of S&P 500 options. Furthermore, it affects the risk-neutral distribution of variance through the

⁹The term "asymmetric volatility" refers to the fact that the volatility of the VIX is not merely stochastic but also varies asymmetrically in response to changes in the VIX (Park (2016)).

¹⁰For parsimony and ease of identification, I allow only the negative price jumps to impact the V and Z .

co-jumps in V and Z , which can improve the model fit of VIX options, as well.

3.2. Nested specification

The model presented above is quite general, and it subsumes existing pricing models along many dimensions. For the two-factor setting, with Z and U absent and excluding volatility jumps, we obtain the Bates (2000) jump-diffusion. I label this model 2F (for two-factor model).¹¹ I further add co-jumps in the model, denoted 2F-CJ (two-factor with co-jumps). Co-jumps have been shown to be critical for fitting the S&P option surface, as Broadie et al. (2007) has noted. Its effect on joint modeling of S&P 500 and VIX options, however, has not yet been investigated in depth.

Next, I study the three-factor setting, with either Z or U absent. The model, including factor U and co-jumps, is labeled 3FU-CJ. This model has been applied in Andersen et al. (2015).¹² The authors show that the 3FU-CJ model outperforms other nested models in fitting S&P 500 options. Bardgett et al. (2019) also apply this model to infer the volatility dynamics from S&P 500 and VIX markets. I extend their work by thoroughly comparing the model with other models and by fitting the model with a longer sample period. I then investigate the model with factors V , m , and Z . The model also includes both independent and contemporaneous jumps in factor V and is labeled 3FZ-ICJ. The inclusion of the new Z factor is the main departure from prior works. The importance of stochastic volatility of volatility for pricing VIX options has been noted in Mencía and Sentana (2013) and Park (2016). They, however, study a reduced model without incorporating the information from S&P 500 options. Branger et al. (2016) also include a volatility-of-volatility factor in the consistent model. However, they estimate the model with VIX options data only. Furthermore, their model cannot capture the leverage effect and asymmetric volatility property.

[Insert Table 3 near here]

I then consider the four-factor setting, with both Z and U included. To investigate the importance of co-jumps, I first study a four-factor model that includes only independent volatility jumps

¹¹This study excludes a one-factor jump-diffusion model, with m , Z and U absent, studied in Pan (2002) and Broadie, Chernov, and Johannes (2007) Christoffersen et al. (2009) show that the two-factor model significantly outperforms the single-factor model for pricing S&P 500 options. Importantly, the m factor is needed to price VIX futures and options (Mencía and Sentana (2013)). I also include return jumps in all models analyzed in this paper.

¹²Andersen et al. (2015) assume that U_t is driven by a pure jump process. I also test their specification. The resulting implications are similar and available upon request. Therefore, consistent with Bardgett et al. (2019), I assume that U_t is only driven by a diffusion process.

and is labeled 4F-IJ. Finally, I extend the 4F-IJ model by including co-jumps, resulting in a full specification model characterized by Equations (1) - (5). The model is labeled 4F-ICJ. The details of model specifications are summarized in Table 3.

3.3. Derivatives pricing

Given the model specification, I first derive the expression of the VIX, which is defined as a finite sum of call and put prices that converges on the integral $VIX_t^2 = \frac{2}{T-t} \mathbb{E}_t^{\mathbb{Q}} \left[\int_t^T \frac{dF_s}{F_{s-}} - d(\ln F_s) \right]$, where $T - t$ is 30 days in annual terms.

Proposition 1. *Under the model specification given in Equations (1) - (5), the VIX squared at time t can be written as an affine deterministic function of the risk factors:*

$$\begin{aligned} VIX_t^2 &= \frac{1}{T-t} \mathbb{E}_t^{\mathbb{Q}} \left[\int_t^T V_s ds + 2 \int_t^T \int_{\mathbb{R}^2} (e^x - 1 - x) \mu(dx, ds) \right] \\ &= A_{VIX^2} + B_{VIX^2}^{\top} \mathcal{V}_t, \end{aligned} \tag{10}$$

and this gives us

$$VIX_t = \sqrt{A_{VIX^2} + B_{VIX^2}^{\top} \mathcal{V}_t}, \tag{11}$$

where \mathcal{V}_t represents state vector at time t , and the coefficients A_{VIX^2} and B_{VIX^2} are known in closed form and provided in Appendix A.

The models in this study belong to the class of affine models. Therefore, derivatives pricing is most efficiently performed using Fourier inversion techniques. To apply the techniques, I first derive the characteristic function of the underlying processes.

Proposition 2. *Under the model specification given in Equations (1) - (5), the characteristic*

function of logarithm of S&P 500 and VIX squared are exponential affine of the risk factors

$$\begin{aligned}\phi_{S_T}(t, \mathcal{V}_t; u) &= \mathbb{E}_t^{\mathbb{Q}} \left[e^{iu \log(S_T)} \right] \\ &= e^{-\alpha(\tau) - \beta(\tau) \log(S_t) - \gamma(\tau) V_t - \psi(\tau) m_t - \xi(\tau) Z_t - \varpi(\tau) U_t},\end{aligned}\quad (12)$$

$$\begin{aligned}\phi_{VIX_T^2}(t, \mathcal{V}_t; u) &= \mathbb{E}_t^{\mathbb{Q}} \left[e^{iu VIX_T^2} \right] \\ &= e^{-\alpha_{VIX^2}(\tau) - \gamma_{VIX^2}(\tau) V_t - \psi_{VIX^2}(\tau) m_t - \xi_{VIX^2}(\tau) Z_t - \varpi_{VIX^2}(\tau) U_t},\end{aligned}\quad (13)$$

where \mathcal{V}_t represents risk factors at time t . The conditional characteristics function can be quasi-analytically calculated by solving a system of Riccati ordinary differential equations (ODEs) which are given in Appendix B.

VIX futures and options written on the forward VIX. Thus, the price of futures with a maturity of T at time t is equal to the risk-neutral expectation of the forward VIX

$$F_{VIX}(t, T) = \mathbb{E}_t^{\mathbb{Q}} \left[\sqrt{VIX_T^2} \right]. \quad (14)$$

The payoff of a call option on the VIX with maturity in T and strike price K is the maximum value between $VIX_T - K$ and 0. Based on the risk-neutral pricing theory, we can express the value of a European call option as

$$C_{VIX}(t, T, K) = \mathbb{E}_t^{\mathbb{Q}} \left[e^{-\int_t^T r_s ds} \left(\sqrt{VIX_T^2} - K \right)^+ \right]. \quad (15)$$

As shown in Equation (11), VIX is a nonlinear function of the risk factors. This makes the pricing of derivatives on the VIX more involved. Following Branger et al. (2016), I deal with this nonlinearity by transforming the payoff function and rely on the Fourier inversion techniques in Lewis (2000) and Chen and Joslin (2012).

Proposition 3. *Given the fundamental transform, a generalization of the characteristic function that allows complex arguments is available. The Fourier transform of the payoff function can be*

applied to price derivatives. The price of a call option on the VIX can be solved by¹³

$$\begin{aligned} C_{VIX}(t, T, K) &= \mathbb{E}_t^{\mathbb{Q}} \left[e^{-\int_t^T r_s ds} \left(\sqrt{VIX_T^2} - K \right)^+ \right] \\ &= \frac{e^{-r\tau}}{\sqrt{\pi}} \int_0^\infty \mathcal{R} \left[\phi_{VIX_T^2}(t, \mathcal{V}_t; -(z_r + iz_i)) \frac{(1 - \text{erf}(K\sqrt{z_i - iz_r}))}{2(z_i - iz_r)^{3/2}} \right] dz_r, \end{aligned} \quad (16)$$

and the future price can be calculated by

$$\begin{aligned} F_{VIX}(t, T) &= \mathbb{E}_t^{\mathbb{Q}} \left[\sqrt{VIX_T^2} \right] \\ &= \frac{1}{\sqrt{\pi}} \int_0^\infty \mathcal{R} \left[\phi_{VIX_T^2}(t, \mathcal{V}_t; -(z_r + iz_i)) \frac{1}{2(z_i - iz_r)^{3/2}} \right] dz_r, \end{aligned} \quad (17)$$

where $\tau = T - t$, and z_r and z_i denote the real and imaginary parts of complex variable z . erf denotes the error function of a complex-valued argument. $\mathcal{R}[z]$ denotes the real part of z . Details on the computation are provided in Appendix C.

3.4. Estimation

I now estimate the joint model on S&P 500 and VIX options. The development of formal tools for parametric inference in the context of an options panel is challenging. Several approaches for estimating pricing models have been proposed in the literature. One popular approach is to filter latent states using the time series of underlying returns, which ensures consistency between the physical and risk-neutral measures. This is done in a Bayesian setting in Jones (2003) and Eraker et al. (2003). Andersen, Benzoni, and Lund (2002) and Chernov and Ghysels (2000) use an Efficient Method of Moments approach, Pan (2002) uses the Generalized Method of Moments, Carr and Wu (2007) and Mencía and Sentana (2013) use a Kalman filter approach, and Johannes, Polson, and Stroud (2009), Fulop, Li, and Yu (2015) and Bardgett et al. (2019) use particle filtering.

Another approach treats the latent states as parameters to be estimated daily and thus avoids filtering the latent factors. This strategy has been widely adopted by Bates (2000), Huang and Wu (2004), Christoffersen et al. (2009), Andersen et al. (2015) and among others. Given the scope of our empirical exercise, I follow this approach. One important feature of this approach is that the

¹³Assuming that interest rate is constant, represented by r .

estimation procedure can be largely paralleled, which significantly facilitates the joint estimation on S&P 500 and VIX options.¹⁴

I denote the structural parameters of the 4F-ICJ model by Θ and state vector at time t by $\mathcal{V}_t = (V_t, m_t, Z_t, U_t)$. Further, the model-implied Black-Scholes IV is given by $IV_X(t, T, K, \mathcal{V}_t, \Theta)$, where X represents the underlying asset and K is the strike price. For simplicity, thereafter, I use IV_X to represent $IV_X(t, T, K, \mathcal{V}_t, \Theta)$. The estimation proceeds by jointly optimized over parameters and state vector realizations. The procedure mainly involves two parts: structural parameters optimization and states optimization.

Structural parameters optimization. To estimate the structural parameters, I construct an estimator which takes form¹⁵

$$\hat{\Theta} = \arg \min \frac{1}{2} (\text{error}_{\text{SPX}} + \text{error}_{\text{VIX}}), \quad (18)$$

where error_X is defined as¹⁶

$$\text{error}_X = \frac{1}{N_X} \sum_{n,t}^{N_X} \left(\frac{IV_X(t, n) - IV_X^M(t, n)}{IV_X^M(t, n)} \right)^2, \quad X \in \{\text{SPX}, \text{VIX}\}, \quad (19)$$

where $N_X = \sum_{t=1}^T N_X(t)$. $N_X(t)$ denotes the total number of option contracts at time t . IV_X^M represents the market-implied volatilities.

States optimization. For a given set of structural parameters, Θ , I trivially obtain the corresponding state vector \mathcal{V}_t by solving T equal-weighted pricing error optimization problems of the form

$$\mathcal{V}_t = \arg \min \frac{1}{2} (\text{error}_{\text{SPX}}(t) + \text{error}_{\text{VIX}}(t)), \quad t = 1, 2, \dots, T, \quad (20)$$

¹⁴In theory, the entire system can be identified and estimated consistently from a single cross-section. However, the identification from a single option surface is week. The use of a large number of surface allows the variation in the state vector over time to assist in identifying the underlying structure governing the option prices (Andersen et al. (2015)).

¹⁵I exclude pricing errors of VIX futures from the object function as I obtain the futures price directly from VIX options. I also find that all models price VIX futures reasonably well.

¹⁶I use relative implied volatility to avoid putting too much weight on highly volatile periods.

where $\text{error}_X(t)$ is defined as

$$\text{error}_X(t) = \frac{1}{N_X(t)} \sum_{n=1}^{N_X(t)} \left(\frac{IV_X(t, n) - IV_X^M(t, n)}{IV_X^M(t, n)} \right)^2, \quad X \in \{\text{SPX}, \text{VIX}\}. \quad (21)$$

In order to ensure that the estimation is not dominated by one data set, I equally weight the pricing errors. Furthermore, I use root mean square relative errors as the magnitude of IV_{VIX} is significantly larger than that of IV_{SPX} . One benefit of this estimation procedure is that the daily estimation over state vectors $\{\mathcal{V}_t\}_{t=1,2,\dots,T}$ can be largely paralleled. Furthermore, to accelerate the computation, I utilized CUDA to offload the highly numerical-demanding part to the Graphics Processing Unit (GPU). Finally, I use a global optimizer, namely the Covariance Matrix Adaptation Evolution Strategy (CMA-ES), introduced by Hansen and Ostermeier (1996), to cope with the non-convexity of the calibration problem and the potential existence of multiple local minima.

4. Parameter Estimates

4.1. In-sample versus out-of-sample

As a starting point, I compare the data distribution in the in-sample and out-of-sample periods.¹⁷

[Insert Figure 5 near here]

Figure 5 displays scatter plots of skew and ATM IV for both short-term and long-term options. Panels A and B show the results of S&P 500 options. The most distinct feature is that the out-of-sample data points concentrate on low-ATM IV and low-skew space. In-sample data points, however, show some extreme values in the right-up corner. Most of these extreme values are generated during the 2008 financial crisis.

Panels C and D show the results of VIX options. Interestingly, there are almost no extreme values for the short-term scatter plot. Furthermore, for the short-term IVs, the distribution of out-of-sample points is similar to that of in-sample data points. Panel D, however, displays a distinct pattern for both in- and out-of-sample periods. It is notable that in-sample data points mainly exist

¹⁷I emphasize that I randomly choose the cut-off point to split the full sample period into in-sample and out-of-sample periods.

in low-ATM IV and low-skew areas, and some extreme values even appear in the far left-bottom space. Importantly, the out-of-sample points, however, concentrate on high-ATM IV and high-skew areas, indicating that investors worry about rapid increases in long-term volatility even during the high volatility-of-volatility period. The distinct differences between in- and out-of-sample periods therefore pose a challenge to the pricing models. A successful model should perform well during both periods. The differences can also help us investigate the effects of different model features on IV surfaces.

4.2. In-sample parameter estimates

Table 4 reports in-sample point estimates and standard errors resulting from the estimation of the 2F, 2F-CJ, 3FU-CJ, 3FZ-ICJ, 4F-IJ, and 4F-ICJ specifications.

[Insert Table 4 near here]

As expected, V is highly mean-reverting toward m , which in turn mean-reverts rather more slowly to its long-run mean θ_m . The speed of mean reversion of V , however, is highly dependent on the model specification. The estimated k_v of models without factor U has the highest value, ranging from 13.689 to 18.778. The models that include U have a lower value of k_v , ranging from 3.569 in the 4F-IJ model to 8.225 in the 3FU-CJ model. V also has a high volatility parameter σ_v , which has the highest value, 2.525, in 2F and the lowest value, around 0.48, in four-factor models. Furthermore, adding co-jumps in 2F can decrease σ_v to 1.056. Not surprisingly, I continue to find a prominent leverage coefficient, ρ_1 , across all models. Importantly, the highly statistically significant estimates of ς indicate that Z contributes to the diffusion part of V .

The estimated speed of mean reversion of m is stable among different model specifications ($0.932 < k_m < 1.731$). Therefore, V captures transitory shocks, whereas m is persistent and captures smoother medium- to long-term trends. The estimated volatility of m has the highest value, 0.115, in 2F, and has a much lower value, ranging from 0.006 to 0.015, across other models. The dynamics of Z differ, depending on the model specifications. The speed of mean reversion k_z is highest in the three-factor model. It has the lowest value, 0.013, in the 4F-ICJ model. The 4F-IJ model ($k_z = 0.315$) falls in between. The volatility parameter σ_z is relatively stable across different models. Furthermore, Z is the highest volatile factor as σ_z is between 3.121 to 5.038. Notably, ρ_2

is estimated to be highly positive with a small number of standard errors, indicating the existence of asymmetric volatility property. The highly statistically significant estimates of η_2 also indicate that the models also identify the co-jumps in Z .

The estimated parameters controlling the dynamics of U are stable across different models, and their values are also similar to those estimated in Andersen et al. (2015). The low speed of mean reversion implies that relatively long-term options identify the dynamics of U . Jump-size estimates are statistically significant, with a negative part that captures the value given to large and rare events, with a mean of -11.7% . Bardgett et al. (2019) also estimate a negative jump size of around -11% . The models also identify significant positive jumps in returns, with a mean of 1.6% . Furthermore, jump-size estimates of the independent jumps in V are highly dependent on whether co-jumps are included. Specifically, the 4F-IJ model has the largest jump size, 18.5% , whereas the 3FZ-ICJ and 4F-ICJ models that also include co-jumps have a value of around 9.4% on average. Consistent with Bardgett et al. (2019), I find that the intensity of jumps in returns is time-varying and driven by V and U .

Finally, the estimated parameters of the 3FU-CJ model are very similar to their counterparts in the 4F-ICJ model, except for η_1 . η_1 in the 3FU-CJ model is estimated as 3.511 , which means the volatility jumps are significantly larger than return jumps. As such, the fit with VIX options is heavily dependent on the jump intensity of co-jumps (e.g., V and U). η_1 , however, largely decreases to 1.865 when the model includes Z . Z partially takes over the pivotal role of V and U . As a result, V and U become more flexible to capture the features of S&P 500 options. Including Z can therefore indirectly improve the performance of pricing S&P 500 options. Section 6 provides a detailed analysis of the model's properties.

5. Pricing Performances

5.1. In-sample option panel fit

Data from April 4, 2007 to April 1, 2015 are used for in-sample estimation; the remaining sample data, from April 7, 2015 to December 27, 2017, are used for out-of-sample checks. I use Root Mean Square Relative Errors (RMSREs), as the primary metric to compare the pricing performances of different models. This treatment is aligned with Christoffersen and Jacobs (2004), who emphasize

the importance of using the same criterion for both model identification and evaluation.

[Insert Table 5 near here]

Table 5 reports the overall RMSREs for both in-sample and out-of-sample periods. I consider the two-factor model with co-jumps, denoted 2F-CJ, as the benchmark model, as this model has been studied extensively in the literature. I therefore further report the percentage change of RMSREs in comparison with the benchmark model. There are several noteworthy results. First and foremost, volatility jumps are critical for the joint valuation model. Because by excluding volatility jumps, the pricing error of the 2F model significantly increases by 32.77% in-sample and 23.78% out-of-sample. Second, the three-factor model with either U or Z can largely reduce the pricing errors in both in- and out-of-sample periods. Furthermore, U is relatively more critical during the out-of-sample period. Later, I will show that this is because U can better capture high-volatility-of-volatility and high-volatility skew features during the out-of-sample period. Third, simultaneously including both Z and U can significantly reduce RMSREs by 23.66% in-sample and 31.64% out-of-sample. As a result, the 4F-ICJ model is the most successful model for jointly pricing S&P 500 and VIX options. And fourth, co-jumps are the crucial feature in four-factor models. The 4F-IJ model, which only includes independent jumps in volatility, performs poorly, especially during the out-of-sample period. I will show that this is also because of the vital role of U in capturing high-ATM IV and high-skew for VIX options during the out-of-sample period.

Next, I perform a detailed analysis of the pricing errors by separately checking RMSREs of S&P 500 and VIX options. I also check the RMSREs for each bin by sorting the options by moneyness (K/F) and days to maturity (DTM). Then, to test the statistical significance of the performance difference between different models, I make pairwise model comparisons. Let $D_{i,j,t}$ be the difference of daily RMSRE on time t between models i and j ,

$$D_{i,j,t} = \text{RMSRE}_{i,t} - \text{RMSRE}_{j,t}. \quad (22)$$

Next, I define a test statistic between modes i and j as

$$z_{i,j} = \frac{\overline{D_{i,j,t}}}{\text{stddev}(D_{i,j,t})}, \quad (23)$$

where $\overline{D_{i,j,t}}$ denotes the sample average and $\text{stdev}(\cdot)$ denotes the standard error of the sample mean difference. I adjust the standard error calculation for serial dependence based on Newey and West (1987), with the number of lags optimally chosen based on Andrews (1991) and an AR(1) specification. The test statistic in Equation (23) follows a standard normal distribution under the null hypothesis that there is no statistically significant difference between modes i and j .

[Insert Table 6 near here]

Table 6 reports the results of the in-sample estimates. Panels A and B present the RMSREs of the model IVs for S&P 500 and VIX options, respectively. Panels A.1 and B.1 provide the overall pricing performance of each model specification. Notably, compared to the benchmark, the 4F-ICJ model substantially improves the pricing of S&P 500 options by 15.07% and improves the pricing of VIX options by 31.70%. The improvement is thus most noticeable for VIX options. Furthermore, in Panel A.2, we can observe the reduction of RMSREs for S&P 500 options across all moneyness bins, except for those that are deepest in the money ($1.03 \leq k$). The 4F-ICJ model also improves the model fit with S&P 500 options across all DTM bins, as shown in Panel A.3. The results from Panels B.2 and B.3 show that the 4F-ICJ model significantly improves the performance of the modeling of VIX options along both the moneyness and term structure dimensions. The superior performance of the 4F-ICJ model implies that to capture the features of S&P 500 and VIX options jointly, we need to incorporate both Z and U factors.

Surprisingly, compared with the benchmark, the 4F-IJ model improves the pricing of VIX options significant (by 30.50%) but only improves the pricing of S&P 500 options by 0.65%. This result indicates that the co-jumps play a critical role in the joint valuation model and supports the implication of earlier option pricing models. The inspection of pricing errors of both the 4F-IJ and 4F-ICJ models in Panel A.2 reveals that excluding co-jumps primarily deteriorates the performance of both OTM puts and OTM calls for S&P 500 options.

The result in Table 6 also strongly supports the existence of volatility jumps. This can be seen by comparing the benchmark with the 2F model. The 2F model performs substantially worse both for S&P 500 and VIX options. Specifically, the performance deterioration for S&P 500 options can be observed across all moneyness and days-to-maturity bins. For VIX options, the 2F model has the worst performance of deep OTM calls. For example, the RMSRE of deep OTM VIX calls

$(1.8 \leq k)$ is 0.0619 for the 2F-CJ model, but it increases significantly (to 0.1483) for 2F. Upward volatility jumps therefore help capture the positive skew of VIX IVs. This result is consistent with Mencía and Sentana (2013), Park (2016), and Bardgett et al. (2019). I further complete the option pricing literature on volatility jumps by jointly analyzing the two options markets.

Andersen et al. (2015) introduce factor U to better capture the left tail of the risk-neutral distribution of equity returns. By comparing the 3FU-CJ model with the benchmark, I confirm their findings. Specifically, by introducing U , the 3FU-CJ model improves the model fit by 8.73% for S&P 500 options.¹⁸ Consistent with Bardgett et al. (2019), I also find U can make a large improvement in the pricing of VIX options. As expected, the most considerable improvement stems from the model fit of deep OTM S&P 500 puts and deep OTM VIX calls. This is because U simultaneously controls the jump intensity of negative return jumps and positive volatility jumps.¹⁹

A comparison of pricing errors in the 3FZ-ICJ model and the benchmark uncovers a striking result: including factor Z can improve the performance not only for VIX options but also for S&P 500 options. The result of the 3FU-ICJ model in Panel A.2 shows that Z largely improves the model fit with ATM and moderate OTM S&P 500 options (e.g., $0.9 \leq k < 1.03$). Panel B.2, however, shows that Z substantially improves the fit with deep OTM VIX calls and puts. Panel B.3 indicates that, compared with the benchmark, the decreases of RMSRE in the 3FZ-ICJ model are observed throughout all maturity buckets.

Finally, Panels A.4 and B.4 report pairwise test statistics for S&P 500 and VIX options, respectively. The statistics are in a (6×6) matrix, with the (i, j) th element being the statistic on model i versus model j . Given the symmetry of the test, the diagonal terms are zero by definition, and the lower triangular elements are equal to the negative of the upper triangular elements. Thus, I focus on the lower triangular entries. A negative (positive) statistic in entries (i, j) indicates that model i outperforms (underperforms) model j . The results support the above findings. Most importantly, the 4F-ICJ model statistically and significantly outperforms all other alternative models for both S&P 500 and VIX options.

¹⁸The results of the 3FU-CJ model are comparable to those obtained by Bardgett et al. (2019). They obtain an RMSRE of 9.9%, and I achieve an error of 6.7%. Furthermore, Andersen et al. (2015) report an root-mean-square error (RMSE) of 1.8%. Excluding the financial crisis from the calculation of the RMSREs, I obtain RMSEs of 1.7%, and 2.1% when including the crisis period.

¹⁹I also test the model of which U is fully controlled by a jump process as in Andersen et al. (2015). The pricing errors are very close to those of the 3FU-CJ model and are available upon request.

5.2. Out-of-sample option panel fit

As shown in Equations (1) - (5), the 4F-ICJ model is richly parameterized, which may raise concerns regarding potential in-sample overfitting. I conduct an extensive out-of-sample exercise to corroborate that the improved in-sample fit is due to the improved modeling of features in both S&P 500 and VIX options rather than to a simple increase in the number of model parameters and factors. Broadly speaking, out-of-sample is selected as the never-before-seen dataset. Therefore, if the dynamic features extracted from the option surface though the 4F-ICJ model are genuine and stable, the model should continue to provide a superior fit with the options observed during the out-of-sample period, as well.

[Insert Table 7 near here]

To assess the robustness of the 4F-ICJ model relative to the alternative specifications, I use the parameters for each model estimated over the course of the in-sample period (Table 4) to price the options over the course of the out-of-sample period optimizing only more than the state vector (*States optimization*). Table 7 summarizes the out-of-sample fit with the S&P 500 and VIX options for the various models. Similar to Table 6, Panels A.1 and B.1 provide the overall pricing performance of each model specification. Importantly, I continue to observe that the 4F-ICJ model substantially improves the pricing of both S&P 500 and VIX options on the benchmark and provides superior fits over other alternative specifications. Specifically, compared with the benchmark, the 4F-ICJ model reduces the pricing errors of S&P 500 options by 27.25% and errors of VIX options by 36.04%. The results are striking, as the superiority of the 4F-ICJ model is more pronounced out-of-sample than in-sample.

[Insert Figure 6 near here]

Surprisingly, the 4F-IJ model provides worse fits with both S&P 500 and VIX options. This result further supports the vital role of co-jumps in the joint valuation model. The significant deterioration of the performance for pricing VIX options stems from the unique features of VIX options during the out-of-sample period. As discussed in Section 4.1, the long-term VIX IV surface is fully characterized by high ATM IV and high skew. Such a feature is effectively captured by factor U , which can simultaneously elevate VIX IV and steepen the skew by increasing the jump

intensity of co-jumps. This effect can be observed in Figure 6, where I compare the roles of Z and U in driving the VIX IV surface dynamics. Figure 6 plots the VIX IVs characteristics and their sensitivities with respect to Z and U at the current values of the state vector for each day in the sample. These sensitivities are measured through the change of the characteristics stemming from increases and decreases in factors by 50% from its estimated value. There are several noteworthy observations. First, Z and U play an equally important role in capturing the dynamics of the short-term ATM IV and skew during the in-sample period. Second, Z has a relatively significant impact on the IV skew at the peaks of financial crises. Later, I will show that an increase in Z can elevate the VIX ATM IV but decrease VIX skew. Including Z can therefore effectively capture the negative relation between volatility and volatility skew, especially during financial crises (see, e.g., Figure 3). Third, the effect of U significantly increases at the end of the out-of-sample period, during which both VIX ATM IV and skew have significantly increased. As such, Z and U have distinct yet complementary roles in driving the dynamics of VIX IV surface.

The critical role of U during the out-of-sample period also explains the much better performance of the 3FU-CJ model for fitting VIX options. Although Panel B.4 reports that there is no significant difference between the 4F-ICJ and 3FU-CJ models for pricing VIX options, Panel A.4 shows that the 4F-ICJ model significantly outperforms the 3FU-CJ model for fitting S&P 500 options. As a result, the 4F-ICJ model continues to have a superior performance in the joint pricing framework. Finally and not surprisingly, 2F significantly underperforms the benchmark in the out-of-sample period.

To sum up, I find decisive evidence that Z , U , and co-jumps have enormous and statistically significant effects on the joint valuation of S&P 500 and VIX options. The 4F-ICJ model is strongly preferred to other alternative specifications in both in- and out-of-sample tests.

5.3. Structures in pricing errors

Another way to investigate the performance of different model specifications is to check for remaining structures in the pricing errors of these models. I define pricing errors as the difference between the model-implied IV and the market-observed IV. If a model is specified reasonably well, we should find minimal structures in the pricing errors on the S&P 500 and VIX options. I check for remaining structures in the mean pricing error at each moneyness and maturity. The mean

pricing error of a good model should be close to zero and show no apparent structures along both the moneyness and the maturity dimensions.

Since an option's days to maturity and moneyness change every day, I estimate the pricing error at fixed moneyness and maturity by using nonparametric smoothing. A positive pricing error indicates model overpricing compared to market data, and a negative pricing error indicates model underpricing.

5.3.1. S&P 500 index options analysis

Figure 7 plots the smoothed pricing errors of S&P 500 options at different moneyness and maturities under each of the six model specifications. Within each panel, the five lines represent pricing errors for five maturities: 30 (solid), 60 (dashed), 90 (dotted), 150 (dot-dashed), and 300 days (dash-dash-dotted).

[Insert Figure 7 near here]

Panels A and B show that the two-factor models (2F and 2F-CJ) exhibit large mean pricing errors along with both the maturity and the moneyness dimensions. At short maturities, two-factor models overprice OTM puts relative to OTM calls. At long maturities, the pattern is reversed. OTM puts are underpriced relative to OTM calls. Compared with the 2F model, the 2F-CJ model gradually reduces pricing errors to zero as we move from deep OTM put to ATM options. The 2F model, however, consistently overprices options with K/F smaller than 1.

Consistent with Andersen et al. (2015), I find that including U can substantially improve the model fit on OTM puts, as shown in Panel C. The 3FU-CJ model shows much better performance, except at very long maturities (300 days), where it still significantly underprices OTM puts. The IV skew is a direct result of conditional non-normality in asset returns. The downward slope of the skew reflects asymmetry (negative skewness) in the risk-neutral distribution. The positive curvature of the skew reflects the fat-tails (leptokurtosis) of this distribution. The central limit theorem, moreover, implies that under very general conditions, the conditional return distribution should converge to normality as the maturity increases. As a result, the IV skew should flatten out when the maturity increases. The market data, however, shows that the IV skew steepens slightly

as maturity increases. The biases shown in Panels A to C therefore imply that the IV skew of the corresponding model flattens out faster than observed in the data.

Panel D shows that including Z can increase the curvature of IV smile or kurtosis of risk-neutral distribution. Consistent with Table 6, the 3FZ-ICJ model performs well for ATM options. Furthermore, as shown in Table 4, Z is a persistent factor, which can help to slow down the convergence to normality. Panel E confirms the previous finding that co-jumps is a critical feature of pricing models. The 4F-IJ model consistently underprices OTM puts for medium- to long-term options.

Importantly, Panel F shows that the 4F-ICJ model looks promising in generating a persistent IV skew across the maturity horizon. The mean pricing errors of the 4F-ICJ model are close to zero and show no apparent structures along both the moneyness and the maturity dimensions.

5.3.2. VIX options analysis

Figure 8 plots the smoothed pricing errors of VIX options. Within each panel, the four lines represent pricing errors for five maturities: 30 (solid), 60 (dashed), 90 (dotted), and 120 days (dot-dashed).

[Insert Figure 8 near here]

For comparison, I use the same scale for all panels except for Panel A, where I use a larger scale to accommodate the larger pricing errors from the 2F model. Panel A shows that the 2F model has difficulty capturing the positive IV skew of VIX options across all maturities. The model consistently overprices (underprices) short-term (long-term) options across the moneyness dimension. Volatility jumps are thus a necessary feature for pricing VIX options. The 2F-CJ model, as shown in Panel B, exhibits much better performance. I nonetheless still observe prominent error structures in Panel B. The 2F-CJ model consistently underprices OTM VIX calls across all maturities. The 2F-CJ model is thus still struggling to capture positive IV skew patterns of VIX options.

Panel C illustrates that the positive IV skew can be effectively captured by incorporating U . As a result, the 3FU-CJ model substantially improves the model fit of VIX options. The 3FU-CJ model, however, generates steeper IV skew than observed in the data. The 3FU-CJ model

overprices OTM call options relative to OTM put options. Panel D shows that the 3FZ-ICJ model can largely improve the performance of the 2F-CJ model by including factor Z . Unlike the 3FU-CJ model, the 3FZ-ICJ model generates a relatively flatter IV skew. Furthermore, the 3FZ-ICJ model shows a much better fit with long-term options.

Panel E shows the results of the 4F-IJ model, which incorporates both Z and U but excludes co-jumps in V . As a result, the jump intensity of volatility jumps is driven by V and Z . Factor U , however, has a major impact on return jumps, which can substantially increase the flexibility of the model for pricing S&P 500 options in the joint valuation framework. The limited model's flexibility for pricing S&P 500 options can also deteriorate the performance on VIX options. For example, the model structures or factor levels are forced to capture the features of S&P 500 options at the expense of the fitness of VIX options, and the reverse is also true. Like the 3FZ-ICJ model, the 4F-IJ model also relatively underprices OTM calls. U is therefore crucial for capturing a high skew pattern.

Panel F shows the results of the 4F-ICJ model. As expected, the 4F-ICJ model produces the smallest pricing errors along both the moneyness dimension and the maturity dimension. Compared with the 4F-IJ model, the success of the 4F-ICJ model stems from incorporating co-jumps in V . Consequently, U can directly affect the volatility jumps and thus the risk-neutral distribution of variance. Not surprisingly, including co-jumps can largely improve the model fit on OTM calls across all maturities. As shown in Panel F, the right ends of all of the curves are very close to zero. Combining all the evidence, I conclude that the 4F-ICJ model significantly outperforms all other nested models in jointly pricing S&P 500 and VIX options.

5.4. Fitting the option characteristics

Finally, I investigate the model's success in capturing the dynamics of the option characteristics. This provides us with another way to assess the performance across the different models.

[Insert Figures 9 and 10 near here]

In Figure 9, I plot the characteristics of S&P 500 IVs along with the model-implied fit of the 4F-ICJ model. As expected, the model provides a near-perfect fit with the ATM IV, for both short- and long-term options. Furthermore, the model shows much better performance for long-term

ATM IV for periods of both turmoil and relative tranquility. The bias, however, can be observed for short-term ATM IVs during highly volatile periods (e.g., 2008 financial crisis). The fits with the short- and long-term skew are also satisfactory, although the model tends to underestimate them at peaks of financial crises. Nonetheless, no evidence exists of major systematic biases, and the relative errors are small except for highly volatile periods. The 4F-ICJ model thus fits S&P 500 option characteristics well, in both in- and out-of-sample periods.

[Insert Table 8 near here]

To access the success of the 4F-ICJ mode in capturing the option surface characteristics, I now compare it with the fit provided by the alternative models. The results are presented in Panel A, Table 8. The estimation does not minimize the distance between the observed and model-implied option characteristics. Nevertheless, the 4F-ICJ model provides a superior fit with three out of four S&P 500 option characteristics. Surprisingly, the benchmark model 2F-CJ provides the best fit with short-term ATM IVs. Compared with the benchmark, the 4F-ICJ model substantially improves the fits with long-term ATM IV, short-term skew, and long-term skew by 53.59%, 19.12%, and 21.24%, respectively.

Furthermore, removing co-jumps from the four-factor setting, leading to the 4F-IJ model, produces a significant deterioration in the fit with the IV skew and short-term ATM IV. Interestingly, the 3FZ-ICJ model also generates promising fits with the S&P 500 option characteristics. Consistent with previous findings, the significant improvement of the 3FZ-ICJ model stems from the fits with ATM options. Specifically, the 3FZ-ICJ model also produces the lowest error for short-term ATM IV (0.0083), and, compared with the benchmark, it substantially reduces the error of long-term ATM IV by 45.75%. The 3FU-CJ model also provides a relatively satisfactory fit with the characteristics. On the other hand, it performs poorly with short-term ATM IVs. Finally and unsurprisingly, the 2F model significantly underperforms the benchmark.

Next, I explore the model fit with VIX option characteristics. Figure 10 plots the VIX IV characteristics along with the model-implied fit of the 4F-ICJ model. As expected, the model also provides a near-perfect fit with the ATM IV, for both short- and long-term options. Similar to the fits with S&P 500 ATM IV, the model generally underestimates VIX ATM IV at peaks of financial crises. The model also tends to overestimate the short-term ATM IV during the tranquility periods

of 2014. The fits with the short- and long-term skew are also satisfactory, although the model tends to overestimate the long-term skew at the peak of the 2008 financial crisis. Surprisingly, the model captures the short-term skew during the financial crises quite well. The 4F-ICJ model thus also fits VIX option characteristics reasonably well, for both in- and out-of-sample periods.

I also compare the fit of the 4F-ICJ model with the fit provided by other nested models in Panel B, Table 8. Not surprisingly, the 4F-ICJ model provides a superior fit with each of the four option characteristics. Specifically, the 4F-ICJ model significantly improves on the benchmark, by 35.5% for short-term ATM IV, 30.85% for long-term ATM IV, 46.71% for short-term skew, and 12.68% for long-term skew. We can also observe similar improvements in the 4F-IJ model on the benchmark, except for in long-term skew. Finally, the 3FU-CJ and 3FZ-ICJ models produce similar results. Combing through all of these pieces of evidence, I conclude that the 4F-ICJ model successfully captures IV characteristics for both S&P 500 and VIX options.

6. Model Properties

6.1. The role of risk factors

At this point, I have shown the superior performance of the 4F-ICJ model on the joint pricing of S&P 500 and VIX options. Importantly, the significant improvement of the 4F-ICJ model stems from incorporating Z , U , and co-jumps. I therefore next detail how they affect S&P 500 and VIX IV smiles. In constructing the IV curves, I set the interest rate at its full-sample average and fix the S&P 500 options moneyness from 0.7 to 1.05 and the VIX options moneyness from 0.8 to 1.8.

[Insert Figures 11 and 12 near here]

Figure 11 plots the impact of risk factors Z and U on S&P 500 IV smile for short (30 days) and long (270 days) maturities. The solid lines are the mean IV evaluated at the sample median of each factor. The dotted (dashed) lines in each panel are generated by increasing (decreasing) the corresponding factor by 50% and fixing other factors at their sample median.

Panels A and B show the impact of Z on S&P 500 IVs. Surprisingly, Z has little impacts on S&P 500 IV smiles. An increase in Z only slightly steepens the long-term IV skew. This raises a question: how does the 4F-ICJ model improve the performance on the 3FU-CJ model by including

a new factor Z ? Because Z partially takes over other risk factors for pricing VIX options, making them more flexible for capturing the features of S&P 500 options. Including Z can thus indirectly improve the performance of pricing S&P 500 options. The model parameters are also estimated to fit S&P 500 options better. This is true if the two markets contain different information and 3FU-CJ cannot fully capture their features. To see whether including VIX options has an impact on the valuation of S&P 500 options, I apply the parameters in Table 4 to re-estimate the value of the factors by using only S&P 500 options. The results show that the S&P 500 options' RMSREs of the 4F-ICJ (3FU-CJ) model become 0.0567 (0.0588) in-sample and 0.0588 (0.0648) out-of-sample. The empirical analysis yields the following key results. First, the performance of both models on pricing S&P 500 options has been significantly improved without fitting to VIX options. Specifically, excluding VIX options reduces the RMSREs of the 4F-ICJ (3FU-CJ) model by 9.28% (12.37%) in-sample and 12.63% (21.60%) out-of-sample.²⁰ VIX options thus embed conflicting information contained in S&P 500 options, so including them makes the data structure much more complex. Furthermore, including VIX options has a relatively higher impact on 3FU-CJ than 4F-ICJ model. Therefore, the 4F-ICJ model is more representative. Second, I continue to observe that the 4F-ICJ model performs better. The superiority of the 4F-ICJ model thus also stems from its model structure.

[Insert Figure 13 near here]

Figure 13 plots the differences between the estimated risk factors using both options and S&P500 options only as estimation datasets. Solid lines represent the results of the 4F-ICJ model and dotted lines correspond to the results of the 3FU-CJ model. There are several noteworthy points. First, the estimated trajectories for both V and m are relatively consistent throughout the two estimations in times of market calm and yield different estimates during market turmoil. Therefore, the roles played by V and m are relatively stable. However, the inconsistencies between the two markets can be observed during crises, and thus the two markets embed different information sets. Second, we can observe a significant difference in U for the 3FU-CJ model throughout the sample, implying that U carries different information between the two estimations. Including VIX options significantly

²⁰The performance can be further improved by re-estimating model parameters. For illustration purposes, I directly use the parameters reported in Table 4.

changes the trajectory of U because factor U is needed to capture the features in both markets. Consequently, the 3FU-CJ model is not able to adequately represent both markets. Third, and importantly, the differences in U become relatively more stable for the 4F-ICJ model. Including Z stabilizes the performance of U and, therefore, makes the model more representative of both markets. As a result, Z can also improve performance for pricing S&P 500 options, although it cannot directly affect the S&P 500 IV surface.

Panels C and D in Figure 11 show the impact of U on S&P 500 IVs. Consistent with the findings in Andersen et al. (2015), I find that an increase in U elevates the level and steepens the slope of IV skew. U is therefore essential for pricing OTM S&P 500 put options. Furthermore, U is a relatively high persistent factor, as shown in Table 4. It thus also has a significant impact on long-term options.

Next, I exploit the impacts of risk factors on VIX options. Figure 12 displays the simulation results of VIX options, where I follow the same procedure as in Figure 11 and fix the moneyness from 0.8 to 1.8. Panels A and B show the impact of Z on short- and long-term IVs, respectively. We can observe that an increase in Z can elevate the level but flatten the slope of IV. This feature can significantly improve the fit with VIX options during market turmoil. As shown in Figures 3 and 4, a high S&P ATM IV or skew corresponds to a high VIX ATM IV but a low VIX skew. This feature can also explain the pivotal role played by Z in capturing VIX IV characteristics during financial crises implied in Figure 6. Since Z is a highly persistent factor, it is understandable that Z can also significantly affect long-term IVs.

Panels C and D illustrate the impact of U on short- and long-term VIX IVs, respectively. U controls the jump intensity of positive jumps in V , implying that an increase in U should increase volatility of volatility as well as volatility skew. This is what we observe in Panels C and D. Importantly, this feature makes U play a relatively dominant role at the end of the out-of-sample period during which both long-term VIX ATM IV and skew has significantly increased.

To sum up, the results show, first, that both factors have distinct yet complementary roles in the joint valuation framework. Second, both S&P 500 and VIX options contribute to pinning down the dynamics of U . Third, factor Z can only be identified by including VIX options in the model estimation. The findings further support the importance of the joint valuation model and also imply that VIX options contain valuable information on the dynamic of index risk-neutral

distribution that is not spanned by S&P 500 options. Consequently, the 4F-ICJ model is better able to adequately represent and reconcile the two markets.

6.2. The role of co-jumps in diffusion variance

I have argued that incorporating co-jumps is critical for jointly pricing S&P 500 and VIX options. In Section 5, I compared the pricing performance of the 4F-IJ and 4F-ICJ models, and the empirical results confirm that the 4F-ICJ model provide a better fit. In this section, I investigate how the presence of co-jumps in diffusion variance affects options IV curves by changing the value of η_1 .

[Insert Figure 14 near here]

Figure 14 plots the impact of η_1 on the IV smiles of S&P 500 and VIX options. The solid lines are the mean IV, evaluated by setting η_1 at its estimated value of the 4F-ICJ model in Table 4. The dotted (dashed) lines in each panel are generated by increasing (decreasing) η_1 by 50% and fixing other parameters.

Panels A and B show the impact of η_1 on S&P 500 IVs. As expected, a higher value of η_1 implies a high level of IVs and a steeper skew. This effect, however, is more significant in long-term options. Including co-jumps in diffusion variance V thus helps capture the steep IV curve. Furthermore, as shown in Panel B, incorporating co-jumps can significantly slow down the convergence of the return distribution to normality as the maturity increases. This feature helps to capture the fact that the slope of IV skew remains negative for long-term options.

Panels C and D illustrate the impact of η_1 on VIX IVs. An important finding is that η_1 has a relatively higher impact on VIX IVs than S&P 500 IVs. An increase in η_1 also elevates the level of IVs and steepens the slope of IV skew for short-term options. As a result, including co-jumps in diffusion variance V can better capture the fact that VIX IV smile is highly positively skewed. For long-term options, η_1 has a relatively higher impact on the level of IVs than the slope of IV skew.

6.3. The role of asymmetric volatility

One of the most critical features of the 4F-ICJ model is that it allows the diffusion in V and Z to be correlated. In this section, I explore the impact of the correlation ρ_2 on VIX IVs. Importantly,

I investigate whether allowing a nonzero correlation between diffusions in V and Z can capture the asymmetric volatility property in the VIX market, asking whether the volatility of the VIX varies asymmetrically in response to changes in the VIX. As shown in Panel C, Figure 15, there is a positive relationship between changes in the VVIX and in the VIX, and the volatility of VIX, as measured by the VVIX, tends to increase (decrease) as the VIX increase (decreases). Therefore, the stochastic volatility factor implicit in the VIX options is partially spanned by VIX futures.

[Insert Figure 15 near here]

Panels A and B in Figure 15 depict the impact of ρ_2 on VIX IVs for short- and long-term options, respectively. The solid lines are the IV evaluated by setting ρ_2 at 0. The dotted (dashed) lines in each panel are generated by setting ρ_2 at 0.9 (-0.9) and fixing other parameters. It is evident that ρ_2 has a significant impact on both short- and long-term VIX IVs. Specifically, a higher ρ_2 implies a steeper slope of IV skew. The impact of ρ_2 is also relatively more significant among low-strikes options. A lower ρ_2 corresponds to a flatter slope and a more curved IV smile. Combining all of the evidence from Figures 14 and 15, we can conclude that the positive IV skew can be effectively captured by incorporating volatility jumps and allowing a nonzero correlation between diffusion in V and Z .

Finally, I examine the role of ρ_2 in capturing the positive correlation between VIX and VVIX by conducting the Monte Carlo simulation. Specifically, I simulate the dynamics of states based on Equations (1) - (5) for 500 days. For each day, I generate a range of 30-day VIX options with fixed strikes ($0.8 \leq K/F \leq 1.2$) based on the simulated states and estimated parameters of the 4F-ICJ model in Table 4. Next, the VVIX index can be calculated by

$$\text{VVIX}_t = \sqrt{\frac{2}{T-t} \sum_i \frac{\Delta K_i}{K_i^2} e^{r(T-t)} O_{VIX}(t, T, k_i) - \frac{1}{T-t} \left(\frac{F(t, T)}{K_{\text{ATM}}} - 1 \right)^2}. \quad (24)$$

I then calculate the VIX index based on Equation (11). In the last step, I calculate the correlation between VIX log-returns and VVIX log returns, labeled corr. To get the distribution of simulated correlation, I repeat the simulation 1,000 times. Panel D in Figure 15 shows the result of the Monte Carlo simulation. It is evident that the level of corr is highly dependent on ρ_2 . The simulated corr on average is close to -0.7, -0.2 and 0.6 when ρ_2 is equal to -0.9, 0 and 0.9, respectively. It is

therefore critical to allow the $B_{2,t}$ in V_t and $B_{z,t}$ in Z_t to be correlated, which further supports the importance of introducing a new factor Z_t in the joint valuation model. Importantly, the 4F-ICJ model can still capture the leverage effect, which is driven by the negative correlation between W_t in returns and $B_{1,t}$ in V_t as well as the possibility of simultaneous jumps in the returns and V_t .²¹

7. Conclusion

In this paper, I carry out an extensive analysis of model specifications for the joint valuation of S&P 500 and VIX options and emphasize the model features that are critical for reconciling the two markets. In particular, I extend the pricing model applied in Andersen et al. (2015) and Bardgett et al. (2019) by including a new factor Z_t that partially drives the dynamics of volatility of volatility and volatility jumps intensity. Specifically, the model I propose incorporates two diffusion parts ($B_{1,t}$ and $B_{2,t}$) in the volatility process V_t . The (local) volatility of $B_{1,t}$ is driven by V_t , whereas the (local) volatility of $B_{2,t}$ is controlled by Z_t . By allowing a negative correlation between the diffusion part in returns and $B_{1,t}$ and a positive correlation between the diffusion part in Z_t and $B_{2,t}$, the model can effectively capture both the leverage effect and asymmetric volatility property. Importantly, the proposed model is still within the class of affine models, which facilitates the estimation and the comparison with other alternative affine models.

The empirical analysis shows that incorporating factor Z_t can significantly improve the model performance both in- and out-of-sample. Although factor Z_t primarily affects the risk-neutral distribution of return variance, the pricing improvement results from the better fit not only with VIX options but also with S&P 500 options. This finding implies that the two markets contain different information sets that cannot be adequately represented by the existing model. Including Z_t can thus improve the performance in two ways. First, it enables the model to be more flexible for pricing VIX options and, thus lets other risk factors better capture the features of S&P 500 options. Second, it enables the model structure (including estimated parameters) to be more representative of both markets.

The analysis also concludes that price and volatility co-jumps are critical for the joint valuation

²¹If the diffusion volatility is controlled by Z_t only, and as such there is no $B_{1,t}$ term, we may allow a non-zero correlation between W_t and $B_{2,t}$ to capture the leverage effect. This, however, will make the model non-affine for equity options. Therefore, introducing another diffusion volatility term in V_t enables the model to capture both the leverage effect and asymmetric volatility property, and it can also keep the model within the class of affine models.

framework, which supports the findings of earlier works of studying the S&P 500 market alone, e.g., Bates (2000), Eraker et al. (2003), and Duffie et al. (2000). The co-jumps can be better identified by jointly pricing S&P 500 and VIX options. This is because VIX options portray the conditional density of future VIX levels and, as such, contain more information on the future density of S&P 500 return variance. The empirical results also support the importance of the price tail factor U_t proposed by Andersen et al. (2015). I extend their studies of U_t by jointly analyzing S&P 500 and VIX options. I find that U_t is also critical for capturing VIX options characteristics, especially during high-VIX ATM IV and high-VIX skew periods.

Lastly, I provide a thorough analysis of the model's properties. I first perform several simulation studies to show the distinct yet complementary roles played by factors Z_t and U_t in capturing S&P 500 and VIX IV smirks. Specifically, I construct simulated IV smirks by changing the levels of either one of the factors alone. The result implies that both factors are indispensable for the joint valuation framework. I further illustrate the impact of co-jumps on IV smirks by performing a similar simulation study. The result confirms the previous findings that co-jumps significantly affect both markets. Finally, by conducting a Monte Carlo simulation, I show that the asymmetric volatility property can be effectively captured by allowing a positive correlation between changes in V_t and Z_t , which also supports the superiority of the model I propose in this paper.

Appendix A. Affine models of VIX²

Assume that the process of a k -dimensional state vector \mathcal{V}_t satisfies the following stochastic differential equation under risk-neutral measure \mathbb{Q}

$$d\mathcal{V}_t = \mu(\mathcal{V}_t)dt + \Sigma(\mathcal{V}_t)dB_t + d\bar{J}_t, \quad (\text{A.1})$$

where $\mu(\mathcal{V}_t) \in \mathbb{R}^k$ denotes the instantaneous drift function, B_t denotes a k -dimensional Brownian motion with $\Sigma(\mathcal{V}_t)\Sigma(\mathcal{V}_t)^\top \in \mathbb{R}^{k \times k}$ being the symmetric and positive definite instantaneous covariance matrix, and $d\bar{J}_t$ represents jump martingale increment. I further set $\mu(\mathcal{V}_t) = M + K\mathcal{V}_t$, $M \in \mathbb{R}^k$, $K \in \mathbb{R}^{k \times k}$. Therefore, the expected integrated state is an affine function of the state variables

$$\mathbb{E}_t^{\mathbb{Q}} \left[\int_t^T b_x^\top \mathcal{V}_s ds \right] = B_x(\tau)^\top \mathcal{V}_t + C_x(\tau), \quad (\text{A.2})$$

where $\tau = T - t$, $b_x \in \mathbb{R}^k$, and

$$B_x(\tau) = (e^{K^T \tau} - I) (K^T)^{-1} b_x, \quad (\text{A.3})$$

$$C_x(\tau) = (B(\tau)^T - b_x^\top \tau) K^{-1} M. \quad (\text{A.4})$$

Based on the above results, the VIX squared at time t can be written as an affine deterministic function of risk factors:

$$\begin{aligned} \text{VIX}^2 &= \frac{1}{\tau} \mathbb{E}_t^{\mathbb{Q}} \left[\int_t^T V_s ds + 2 \int_t^T \int_{\mathbb{R}^2} (e^x - 1 - x) \mu(dx, ds) \right] \\ &= \frac{1}{\tau} \mathbb{E}_t^{\mathbb{Q}} \left[\int_t^T b_v^\top \mathcal{V}_s ds + 2 \int_t^T \int_{\mathbb{R}^2} (e^x - 1 - x) \mu(dx, ds) \right] \\ &= \frac{1}{\tau} \left(\mathcal{K} \mathbb{E}_t^{\mathbb{Q}} \left[\int_t^T b_v^\top \mathcal{V}_s ds \right] + 2 E^- \lambda_2^- \mathbb{E}_t^{\mathbb{Q}} \left[\int_t^T b_u^\top \mathcal{V}_s ds \right] \right) + \mathcal{U} \\ &= \frac{1}{\tau} \left(\mathcal{K} \left[B_v(\tau)^\top \mathcal{V}_t + C_v(\tau) \right] + 2 E^- \lambda_2^- \left[B_u(\tau)^\top \mathcal{V}_t + C_u(\tau) \right] \right) + \mathcal{U} \\ &= A_{\text{VIX}^2} + B_{\text{VIX}^2}^\top \mathcal{V}_t, \end{aligned} \quad (\text{A.5})$$

with

$$A_{\text{VIX}^2} = \frac{1}{\tau} (\mathcal{K}C_v(\tau) + 2E^- \lambda_2^- C_u(\tau)) + \mathcal{U}, \quad (\text{A.6})$$

$$B_{\text{VIX}^2} = \frac{1}{\tau} (\mathcal{K}B_v + 2E^- \lambda_2^- B_u), \quad (\text{A.7})$$

where $\mathcal{K} = 1 + 2E^+ \lambda_1^+ + 2E^- \lambda_1^-$, $\mathcal{U} = 2E^+ \lambda_0^+ + 2E^- \lambda_0^-$, and $E^{+/-} = (\delta_1^{+/-})^2 / (1 - \delta_1^{+/-})$.

Appendix B. Characteristic functions

Assume that the characteristic functions of $\log(S_T)$ and VIX^2 take the exponential affine form

$$\begin{aligned} \phi_{S_T}(t, \mathcal{V}_t; u) &= \mathbb{E}_t^{\mathbb{Q}} \left[e^{iu \log(S_T)} \right] \\ &= e^{-\alpha(\tau) - \beta(\tau) \log(S_t) - \gamma(\tau) V_t - \psi(\tau) m_t - \xi(\tau) Z_t - \varpi(\tau) U_t}, \end{aligned} \quad (\text{B.1})$$

$$\begin{aligned} \phi_{\text{VIX}_T^2}(t, \mathcal{V}_t; u) &= \mathbb{E}_t^{\mathbb{Q}} \left[e^{iu \text{VIX}_T^2} \right] \\ &= e^{-\alpha_{\text{VIX}^2}(\tau) - \gamma_{\text{VIX}^2}(\tau) V_t - \psi_{\text{VIX}^2}(\tau) m_t - \xi_{\text{VIX}^2}(\tau) Z_t - \varpi_{\text{VIX}^2}(\tau) U_t}, \end{aligned} \quad (\text{B.2})$$

where $u \in \mathbb{R}$ and i denotes imaginary number. According to the results from *Duffie et al.* (2000), the coefficients in the definition of $\phi_{\text{VIX}_T^2}$ satisfy the following ODEs, with $\tau = T - t$

$$\begin{aligned} \dot{\alpha}_{\text{VIX}^2}(\tau) &= \kappa_m \theta_m \psi(\tau) + \kappa_z \theta_z \xi(\tau) + \kappa_u \theta_u \varpi(\tau) \\ &\quad - \lambda_0^- \left(\frac{1}{(1 - \eta_1 \delta_1^- \gamma(\tau)) (1 - \eta_2 \delta_1^- \xi(\tau))} - 1 \right) - \xi_0 \left(\frac{1}{(1 + \delta_2 \gamma(\tau))} - 1 \right), \\ \dot{\gamma}_{\text{VIX}^2}(\tau) &= -\kappa_v \gamma_{\text{VIX}^2}(\tau) - \frac{1}{2} \sigma_v^2 \gamma_{\text{VIX}^2}^2(\tau) - \lambda_1^- \left(\frac{1}{(1 - \eta_1 \delta_1^- \gamma(\tau)) (1 - \eta_2 \delta_1^- \xi(\tau))} - 1 \right) \\ &\quad - \xi_1 \left(\frac{1}{(1 + \delta_2 \gamma(\tau))} - 1 \right), \\ \dot{\psi}_{\text{VIX}^2}(\tau) &= \kappa_v \gamma_{\text{VIX}^2}(\tau) - \kappa_m \psi_{\text{VIX}^2}(\tau) - \frac{1}{2} \sigma_m^2 \psi_{\text{VIX}^2}^2(\tau), \\ \dot{\xi}_{\text{VIX}^2}(\tau) &= -\kappa_z \xi_{\text{VIX}^2}(\tau) - \frac{1}{2} \varsigma^2 \gamma_{\text{VIX}^2}^2(\tau) - \sigma_z \varsigma \rho_2 \gamma_{\text{VIX}^2}(\tau) \xi_{\text{VIX}^2}(\tau) - \frac{1}{2} \sigma_z^2 \xi_{\text{VIX}^2}^2(\tau) \\ &\quad - \xi_2 \left(\frac{1}{(1 + \delta_2 \gamma(\tau))} - 1 \right), \\ \dot{\varpi}_{\text{VIX}^2}(\tau) &= -\kappa_u \varpi_{\text{VIX}^2}(\tau) - \frac{1}{2} \sigma_u^2 \varpi_{\text{VIX}^2}^2(\tau) - \lambda_2^- \left(\frac{1}{(1 - \eta_1 \delta_1^- \gamma(\tau)) (1 - \eta_2 \delta_1^- \xi(\tau))} - 1 \right), \end{aligned}$$

with boundary conditions $\alpha_{\text{VIX}^2}(0) = iuA_{\text{VIX}^2}$ and $[\gamma_{\text{VIX}^2}(0), \psi_{\text{VIX}^2}(0), \xi_{\text{VIX}^2}(0), \varpi_{\text{VIX}^2}(0)]^\top = iuB_{\text{VIX}^2}$, where the coefficients A_{VIX^2} and B_{VIX^2} are defined in Appendix A.

The coefficients of ϕ_{s_T} satisfy the following ODEs for $t \in (0, T]$

$$\begin{aligned}\dot{\alpha}(\tau) &= \left(r_t - \left(\frac{1}{1 - \delta_1^+} - 1 \right) \lambda_0^+ - \left(\frac{1}{1 - \delta_1^-} - 1 \right) \lambda_0^- \right) \beta(\tau) \\ &\quad + \kappa_m \theta_m \psi(\tau) + \kappa_z \theta_z \xi(\tau) + \kappa_u \theta_u \varpi(\tau) - \xi_0 \left(\frac{1}{(1 + \delta_2 \gamma(\tau))} - 1 \right) \\ &\quad - \lambda_0^- \left(\frac{1}{(1 + \delta_1^- \beta(\tau)) (1 - \eta_1 \delta_1^- \gamma(\tau)) (1 - \eta_2 \delta_1^- \xi(\tau))} - 1 \right) - \lambda_0^+ \left(\frac{1}{(1 + \delta_1^+ \beta(\tau))} - 1 \right) \\ \dot{\beta}(\tau) &= \left(-\frac{1}{2} - \left(\frac{1}{1 - \delta_1^+} - 1 \right) \lambda_1^+ - \left(\frac{1}{1 - \delta_1^-} - 1 \right) \lambda_1^- \right) \beta(\tau) \\ &\quad - \kappa_v \gamma(\tau) - \frac{1}{2} \beta^2(\tau) - \sigma_v \rho_1 \beta(\tau) \gamma(\tau) - \frac{1}{2} \sigma_v^2 \gamma^2(\tau) - \xi_1 \left(\frac{1}{(1 + \delta_2 \gamma(\tau))} - 1 \right) \\ &\quad - \lambda_1^+ \left(\frac{1}{(1 + \delta_1^+ \beta(\tau))} - 1 \right) - \lambda_1^- \left(\frac{1}{(1 + \delta_1^- \beta(\tau)) (1 - \eta_1 \delta_1^- \gamma(\tau)) (1 - \eta_2 \delta_1^- \xi(\tau))} - 1 \right) \\ \dot{\psi}(\tau) &= \kappa_v \gamma(\tau) - \kappa_m \psi(\tau) - \frac{1}{2} \sigma_m^2 \psi^2(\tau) \\ \dot{\xi}(\tau) &= - \left(\frac{1}{1 - \delta_1^-} - 1 \right) \lambda_3^- \beta(\tau) - \kappa_z \xi(\tau) - \frac{1}{2} \zeta^2 \gamma^2(\tau) - \sigma_z \zeta \rho_2 \gamma(\tau) \xi(\tau) - \frac{1}{2} \sigma_z^2 \xi^2(\tau) \\ &\quad - \xi_2 \left(\frac{1}{(1 + \delta_2 \gamma(\tau))} - 1 \right) - \lambda_3^- \left(\frac{1}{(1 + \delta_1^- \beta(\tau)) (1 - \eta_1 \delta_1^- \gamma(\tau)) (1 - \eta_2 \delta_1^- \xi(\tau))} - 1 \right) \\ \dot{\varpi}(\tau) &= - \left(\frac{1}{1 - \delta_1^-} - 1 \right) \lambda_2^- \beta(\tau) - \kappa_u \varpi(\tau) - \frac{1}{2} \sigma_u^2 \varpi^2(\tau) \\ &\quad - \lambda_2^- \left(\frac{1}{(1 + \delta_1^- \beta(\tau)) (1 - \eta_1 \delta_1^- \gamma(\tau)) (1 - \eta_2 \delta_1^- \xi(\tau))} - 1 \right),\end{aligned}$$

with boundary conditions $\alpha(0) = 0$, $\beta(0) = -iu$, $\gamma(0) = 0$, $\psi(0) = 0$, $\xi(0) = 0$, and $\varpi(0) = 0$.

The ODEs can be solved numerically using Runge-Kutta methods. To speed up the computation, I utilize the Graphics Processing Unit (GPU) with the tools provided by NVIDIA CUDA®.

Appendix C. Derivatives pricing

C.1. VIX derivatives pricing

To price futures and options on the VIX, following Branger et al. (2016), I apply the results in Lewis (2000) and Chen and Joslin (2012). Lewis (2000) offers a powerful valuation approach

that is applicable to a wide range of European options. His method requires that the fundamental transform, a generalization of the characteristic function that allows complex arguments, be available. It also requires the Fourier transform of the options payoffs. The forward and inverse Fourier transforms are

$$\begin{aligned}\hat{f}(z) &= \int_{-\infty}^{\infty} e^{izx} f(x) dx \\ f(x) &= \frac{1}{2\pi} \int_{iz_i - \infty}^{iz_i + \infty} e^{-izx} \hat{f}(z) dz,\end{aligned}$$

with transform variable $z = z_r + z_i i$, where z_r and z_i denote the real and imaginary parts of z .

The payoff of a call option on VIX_T is

$$f_1(\text{VIX}_T^2) = \left(\sqrt{\text{VIX}_T^2} - K \right)^+, \quad (\text{C.1})$$

and its forward transform is

$$\hat{f}_1(z) = \frac{\sqrt{\pi} (1 - \operatorname{erf}(K\sqrt{-iz}))}{2(-iz)^{3/2}}, \quad (\text{C.2})$$

where erf denotes the error function of a complex valued argument. A futures contract on VIX_T has the payoff function

$$f_2(\text{VIX}_T^2) = \sqrt{\text{VIX}_T^2}, \quad (\text{C.3})$$

and its forward transform is

$$\hat{f}_2(z) = \frac{\sqrt{\pi}}{2(-iz)^{3/2}}. \quad (\text{C.4})$$

For both payoff functions the Fourier transform is well-behaved if $z_i > 0$. Finally, I get the price of

a call option on VIX_T

$$\begin{aligned}
C_{\text{VIX}}(t, T, K) &= \mathbb{E}_t^{\mathbb{Q}} \left[e^{-\int_t^T r_s ds} \left(\sqrt{\text{VIX}_T^2} - K \right)^+ \right] \\
&= \mathbb{E}_t^{\mathbb{Q}} \left[e^{-\int_t^T r_s ds} f_1(\text{VIX}_T^2) \right] \\
&= \mathbb{E}_t^{\mathbb{Q}} \left[e^{-r\tau} \frac{1}{2\pi} \int_{iz_i-\infty}^{iz_i+\infty} e^{-iz\text{VIX}_T^2} \hat{f}_1(z) dz \right] \\
&= \frac{e^{-r\tau}}{2\pi} \int_{iz_i-\infty}^{iz_i+\infty} \mathbb{E}_t^{\mathbb{Q}} \left[e^{-iz\text{VIX}_T^2} \right] \hat{f}_1(z) dz \\
&= \frac{e^{-r\tau}}{\sqrt{\pi}} \int_0^\infty \mathcal{R} \left[\psi_{\text{VIX}_T^2}(t, \mathcal{V}_t; -(z_r + iz_i)) \frac{(1 - \text{erf}(K\sqrt{z_i - iz_r}))}{2(z_i - iz_r)^{3/2}} \right] dz_r.
\end{aligned} \tag{C.5}$$

Similarly, I get the price of a forward contract on VIX_T

$$\begin{aligned}
F_{\text{VIX}}(t, T) &= \mathbb{E}_t^{\mathbb{Q}} \left[\sqrt{\text{VIX}_T^2} \right] \\
&= \mathbb{E}_t^{\mathbb{Q}} [f_2(\text{VIX}_T^2)] \\
&= \mathbb{E}_t^{\mathbb{Q}} \left[\frac{1}{2\pi} \int_{iz_i-\infty}^{iz_i+\infty} e^{-iz\text{VIX}_T^2} \hat{f}_2(z) dz \right] \\
&= \frac{1}{2\pi} \int_{iz_i-\infty}^{iz_i+\infty} \mathbb{E}_t^{\mathbb{Q}} \left[e^{-iz\text{VIX}_T^2} \right] \hat{f}_2(z) dz \\
&= \frac{1}{\sqrt{\pi}} \int_0^\infty \mathcal{R} \left[\phi_{\text{VIX}_T^2}(t, \mathcal{V}_t; -(z_r + iz_i)) \frac{1}{2(z_i - iz_r)^{3/2}} \right] dz_r,
\end{aligned} \tag{C.6}$$

C.2. S&P 500 options pricing

Although fast Fourier transform (FFT) (e.g., Carr and Madan (1999)) is the most popular method in the literature, I prefer to use the direction integration (DI) approach to take advantage of GPU. Specifically, the call option can be calculated by

$$C_{\text{SPX}}(t, T, K) = \frac{\exp(-\alpha \log(K) - r(T-t))}{\pi} \int_0^\infty \exp(-iu \log(K)) I(u, \alpha) du, \tag{C.7}$$

with an integrand function $I(u, \alpha)$

$$I(u, \alpha) = \frac{\phi_{s_T}(t, \mathcal{V}_t; u - (\alpha + 1)i)}{\alpha^2 + \alpha - u^2 + (2\alpha + 1)iu}. \tag{C.8}$$

In this paper, I set the smoothing parameter, α as 1.2, truncate the upper bound for the integration domain by 300, and use 128 integrand points, resulting in good results.

One advantage of DI over FFT is that I do not need to interpolate option prices over the strikes, leading to a more accurate result with dramatically reduced time. The most important is that with FFT, I have to employ a large number of strikes (e.g., $2^{12} = 4096$), which leads to a broad strike band. However, in most cases, I only need 100 strikes to do the calibration, which means that only 100 of 4096 calculated option prices are really used. Therefore, with DI, I can use the strike vector method to accelerate computation as I only need to calculate characteristic function once for multiple option prices with different strikes.

To further accelerate the computation, I utilize parallel programming on GPU. The main effort is partitioning the computational requirement into thousands of small computations that can be executed simultaneously. These computations are assigned to thousands of threads of the GPU which are executed concurrently on different cores. The GPU hardware consists of a number of streaming multiprocessors which in turn consist of multiple cores. Threads are organized in blocks, where one or more block runs on a streaming multiprocessor (see, e.g., Cook (2012)).

References

- Andersen, Torben G., Luca Benzoni, and Jesper Lund, 2002, An empirical investigation of continuous-time equity return models, *Journal of Finance* 57, 1239–1284.
- Andersen, Torben G., Nicola Fusari, and Viktor Todorov, 2015, The risk premia embedded in index options, *Journal of Financial Economics* 117, 558–584.
- Andrews, Donald, 1991, Heteroskedasticity and autocorrelation consistent covariance matrix estimation, *Econometrica* 59, 817–858.
- Bakshi, Gurdip, Charles Cao, and Zhiwu Chen, 1997, Empirical performance of alternative option pricing models, *Journal of Finance* 52, 2003–2049.
- Bardgett, Chris, Elise Gourier, and Markus Leippold, 2019, Inferring volatility dynamics and risk premia from the s&p 500 and vix markets, *Journal of Financial Economics* 131, 593–618.
- Bates, David S, 2000, Post-'87 crash fears in the S&P 500 futures option market, *Journal of Econometrics* 94, 181–238.
- Branger, Nicole, Alexander Kraftschik, and Clemens Völkert, 2016, The fine structure of variance: Pricing vix derivatives in consistent and log-vix models, Working paper.
- Broadie, Mark, Mikhail Chernov, and Michael Johannes, 2007, Model specification and risk premia: Evidence from futures options, *Journal of Finance* 62, 1453–1490.
- Carr, Peter, and Liuren Wu, 2007, Stochastic skew in currency options, *Journal of Financial Economics* 86, 213–247.
- Chen, Hui, and Scott Joslin, 2012, Generalized transform analysis of affine processes and applications in finance, *Review of Financial Studies* 25, 2225–2256.
- Chernov, Mikhail, and Eric Ghysels, 2000, A study towards a unified approach to the joint estimation of objective and risk neutral measures for the purpose of options valuation, *Journal of Financial Economics* 56, 407–458.

- Christoffersen, Peter, Steven Heston, and Kris Jacobs, 2009, The shape and term structure of the index option smirk: Why multifactor stochastic volatility models work so well, *Management Science* 55, 1914–1932.
- Christoffersen, Peter, and Kris Jacobs, 2004, The importance of the loss function in option valuation, *Journal of Financial Economics* 72, 291–318.
- Chung, San-Lin, Wei-Che Tsai, Yaw-Huei Wang, and Pei-Shih Weng, 2011, The information content of the s&p 500 index and vix options on the dynamics of the s&p 500 index, *Journal of Futures Markets* 31, 1170–1201.
- Cont, Rama, and Thomas Kokholm, 2013, A consistent pricing model for index options and volatility derivatives, *Mathematical Finance* 23, 248–274.
- Cook, S., 2012, *CUDA Programming: A Developer's Guide to Parallel Computing with GPUs*, Applications of GPU Computing Series (Elsevier Science).
- Duffie, Darrell, Jun Pan, and Kenneth Singleton, 2000, Transform analysis and asset pricing for affine jump-diffusions, *Econometrica* 68, 1343–1376.
- Eraker, Bjørn, Michael Johannes, and Nicholas Polson, 2003, The impact of jumps in volatility and returns, *Journal of Finance* 58, 1269–1300.
- Fulop, Andras, Junye Li, and Jun Yu, 2015, Self-exciting jumps, learning, and asset pricing implications, *Review of Financial Studies* 28, 876–912.
- Grünbichler, Andreas, and Francis A. Longstaff, 1996, Valuing futures and options on volatility, *Journal of Banking & Finance* 20, 985–1001.
- Hansen, N., and A. Ostermeier, 1996, Adapting arbitrary normal mutation distributions in evolution strategies: the covariance matrix adaptation, in *Proceedings of IEEE International Conference on Evolutionary Computation*, 312–317.
- Huang, Jing-Zhi, and Liuren Wu, 2004, Specification analysis of option pricing models based on time-changed lévy processes, *Journal of Finance* 59, 1405–1439.

- Johannes, Michael S., Nicholas G. Polson, and Jonathan R. Stroud, 2009, Optimal filtering of jump diffusions: Extracting latent states from asset prices, *Review of Financial Studies* 22, 2759–2799.
- Jones, Christopher S., 2003, The dynamics of stochastic volatility: evidence from underlying and options markets, *Journal of Econometrics* 116, 181–224.
- Kou, S G, 2002, A jump-diffusion model for option pricing, *Management Science* 48, 1086–1101.
- Lewis, Alan L., 2000, *Option Valuation under Stochastic Volatility* (Finance Press).
- Lin, Yueh-Neng, and Chien-Hung Chang, 2010, Consistent modeling of sp 500 and vix derivatives, *Journal of Economic Dynamics and Control* 34, 2302–2319.
- Mencía, Javier, and Enrique Sentana, 2013, Valuation of vix derivatives, *Journal of Financial Economics* 108, 367–391.
- Newey, Whitney K., and Kenneth D. West, 1987, Hypothesis testing with efficient method of moments estimation, *International Economic Review* 28, 777–787.
- Pan, Jun, 2002, The jump-risk premia implicit in options: evidence from an integrated time-series study, *Journal of Financial Economics*. 63, 3–50.
- Park, Yang-Ho, 2016, The effects of asymmetric volatility and jumps on the pricing of vix derivatives, *Journal of Econometrics* 192, 313–328.
- Sepp, Artur, 2008, Pricing options on realized variance in the heston model with jumps in returns and volatility, *Journal of Computational Finance* 11, 33–70.

Table 1: S&P 500 options data summary, April 4, 2007 - December 27, 2017 (557 weeks). Daily settlement prices of S&P 500 options quotes are obtained from OptionMetrics. Moneyness is defined as the strike to future price ratio, $k = K/F(t, T)$. Days-to-maturity (DTM) is in the number of actual days. The implied volatilities are calculated using the Black-Scholes formula.

DTM	< 20	20 - 30	30 - 50	50 - 60	60 - 90	90 - 180	> 180	All
Panel A: Number of option contracts								
$k < 0.8$	874	4560	6837	5061	6540	8200	5946	38018
$0.85 \leq k < 0.90$	2634	5849	3147	6141	3437	2848	1689	25745
$0.90 \leq k < 0.93$	4052	5375	2388	5196	2727	2056	1300	23094
$0.93 \leq k < 0.95$	3958	4689	1832	4066	2028	1434	802	18809
$0.95 \leq k < 0.98$	7417	8266	3049	6390	2969	2199	1263	31553
$0.98 \leq k < 1.00$	5171	5420	2412	4150	2111	1644	971	21879
$1.00 \leq k < 1.03$	7549	8793	3177	6670	3091	2358	1603	33241
$1.03 \leq k$	3126	6299	6782	10150	6401	6640	5338	44736
All	34781	49251	29624	47824	29304	27379	18912	237075
Panel B: Average option prices								
$k < 0.8$	1.09	1.00	1.70	2.18	3.18	5.97	14.85	4.28
$0.85 \leq k < 0.90$	1.16	1.80	9.00	3.72	5.76	17.89	41.69	11.57
$0.90 \leq k < 0.93$	1.57	3.23	14.15	6.34	9.28	25.66	55.19	16.49
$0.93 \leq k < 0.95$	2.44	5.08	19.58	9.31	13.10	33.04	64.05	20.94
$0.95 \leq k < 0.98$	4.99	9.09	28.04	14.80	20.36	43.10	77.57	28.28
$0.98 \leq k < 1.00$	12.05	18.31	41.36	25.75	32.17	57.03	94.28	40.13
$1.00 \leq k < 1.03$	7.27	11.01	31.68	17.01	22.62	47.87	87.60	32.15
$1.03 \leq k$	2.02	2.36	7.57	4.01	4.93	13.28	29.38	9.08
All	4.07	6.48	19.14	10.39	13.93	30.48	58.08	20.37
Panel C: Average option implied volatilities								
$k < 0.8$	0.55	0.37	0.38	0.33	0.33	0.31	0.31	0.37
$0.85 \leq k < 0.90$	0.33	0.27	0.24	0.26	0.24	0.23	0.23	0.26
$0.90 \leq k < 0.93$	0.26	0.22	0.21	0.22	0.21	0.21	0.22	0.22
$0.93 \leq k < 0.95$	0.21	0.19	0.19	0.19	0.18	0.19	0.20	0.19
$0.95 \leq k < 0.98$	0.17	0.16	0.17	0.17	0.16	0.18	0.19	0.17
$0.98 \leq k < 1.00$	0.14	0.13	0.16	0.15	0.15	0.17	0.19	0.15
$1.00 \leq k < 1.03$	0.11	0.11	0.14	0.12	0.12	0.15	0.18	0.13
$1.03 \leq k$	0.19	0.13	0.14	0.15	0.13	0.15	0.16	0.15
All	0.24	0.20	0.20	0.20	0.19	0.20	0.21	0.21

Table 2: VIX options data summary, April 4, 2007 - December 27, 2017 (557 weeks). Daily settlement prices of VIX options quotes are obtained from OptionMetrics. Moneyness is defined as the strike to future price ratio, $k = K/F(t, T)$. Days-to-maturity (DTM) is in the number of actual days. The implied volatilities are calculated using the Black-Scholes formula.

DTM	< 30	30 - 60	60 - 90	90 - 120	> 120	All
Panel A: Number of option contracts						
$k < 0.8$	98	346	409	436	361	1650
$0.8 \leq k < 0.9$	448	870	712	597	387	3014
$0.9 \leq k < 1.0$	828	915	698	591	385	3417
$1.0 \leq k < 1.2$	1736	1627	1409	1347	902	7021
$1.2 \leq k < 1.4$	1164	1393	1215	1190	879	5841
$1.4 \leq k < 1.6$	694	1114	948	1139	967	4862
$1.6 \leq k < 1.8$	301	757	663	805	674	3200
$1.8 \leq k$	156	694	732	883	733	3198
All	5425	7716	6786	6988	5288	32203
Panel B: Average option prices						
$k < 0.8$	0.43	0.49	0.57	0.66	0.74	0.58
$0.8 \leq k < 0.9$	0.59	0.81	1.09	1.25	1.44	1.04
$0.9 \leq k < 1.0$	1.09	1.72	2.10	2.40	2.61	1.98
$1.0 \leq k < 1.2$	1.12	1.76	2.18	2.43	2.69	2.04
$1.2 \leq k < 1.4$	0.63	1.06	1.36	1.59	1.75	1.28
$1.4 \leq k < 1.6$	0.41	0.69	0.91	1.08	1.20	0.86
$1.6 \leq k < 1.8$	0.29	0.48	0.65	0.77	0.86	0.61
$1.8 \leq k$	0.22	0.32	0.41	0.51	0.58	0.41
All	0.60	0.92	1.16	1.34	1.48	1.10
Panel C: Average option implied volatility						
$k < 0.8$	0.99	0.76	0.65	0.59	0.54	0.71
$0.8 \leq k < 0.9$	0.85	0.71	0.65	0.60	0.57	0.68
$0.9 \leq k < 1.0$	0.86	0.78	0.71	0.66	0.61	0.73
$1.0 \leq k < 1.2$	1.02	0.89	0.79	0.72	0.66	0.82
$1.2 \leq k < 1.4$	1.21	1.00	0.88	0.79	0.72	0.92
$1.4 \leq k < 1.6$	1.36	1.10	0.95	0.85	0.76	1.00
$1.6 \leq k < 1.8$	1.46	1.18	1.01	0.89	0.80	1.07
$1.8 \leq k$	1.55	1.30	1.11	0.97	0.86	1.16
All	1.16	0.96	0.84	0.76	0.69	0.88

Table 3: Summary of Model specifications. Models are listed along rows. Columns represent the modeling features. The asterisk indicates that the model includes corresponding features in the column. The features include state vector $\mathcal{V} = (V, m, Z, U)$, independent jumps (IJ) in V , and co-jumps (CJ) in returns and state factors.

	V	m	Z	U	IJ	CJ
2F	*	*				
2F-CJ	*	*				*
3FU-CJ	*	*		*		*
3FZ-ICJ	*	*	*		*	*
4F-IJ	*	*	*	*	*	
4F-ICJ	*	*	*	*	*	*

Table 4: In-sample model parameter estimates. This table reports the model parameter estimates and their standard errors (in parentheses). Models are estimated using S&P 500 and VIX options data sampled every Wednesday over the period April 4, 2007, to April 1, 2015.

	2F	2F-CJ	3FU-CJ	3FZJCJ	4FIJ	4FICJ
κ_v	18.778 (1.324)	13.698 (4.191)	8.225 (0.063)	18.596 (0.069)	3.569 (0.008)	5.878 (0.043)
σ_v	2.525 (0.045)	1.056 (0.147)	0.691 (0.007)	0.680 (0.002)	0.474 (0.001)	0.487 (0.023)
ρ_1	-0.852 (0.007)	-0.956 (0.340)	-0.963 (0.007)	-0.999 (0.002)	-0.868 (0.094)	-0.961 (0.054)
η_1		4.608 (0.637)	3.038 (0.023)	3.511 (0.019)		1.865 (0.101)
ζ				0.021 (0.000)	0.583 (0.001)	0.360 (0.002)
κ_m	1.731 (0.020)	1.449 (0.274)	1.595 (0.012)	0.932 (0.003)	1.020 (0.040)	1.684 (0.076)
θ_m	0.029 (0.000)	0.012 (0.000)	0.009 (0.000)	0.009 (0.000)	0.023 (0.000)	0.022 (0.000)
σ_m	0.115 (0.002)	0.015 (0.001)	0.015 (0.000)	0.006 (0.000)	0.015 (0.002)	0.010 (0.001)
κ_z				1.419 (0.004)	0.315 (0.002)	0.013 (0.001)
σ_z				3.121 (0.012)	5.038 (0.011)	3.239 (0.287)
ρ_2			0.910 (0.005)	0.930 (0.003)	0.900 (0.002)	
η_2				1.712 (0.006)		0.270 (0.016)
κ_u			0.375 (0.003)		0.740 (0.002)	0.318 (0.021)
σ_u			0.461 (0.002)		0.492 (0.000)	0.494 (0.001)
δ_1^-	-0.042 (0.001)	-0.142 (0.014)	-0.082 (0.001)	-0.214 (0.001)	-0.111 (0.001)	-0.109 (0.000)
δ_1^+	0.017 (0.001)	0.016 (0.002)	0.018 (0.000)	0.016 (0.000)	0.016 (0.001)	0.017 (0.000)
δ_2				0.092 (0.006)	0.185 (0.001)	0.096 (0.028)
λ_1^+	0.060 (0.001)	1.144 (0.647)	0.825 (0.007)	1.103 (0.004)	0.190 (0.001)	0.213 (0.008)
λ_1^-	4.962 (0.035)	4.976 (0.647)	2.757 (0.021)	4.999 (0.004)	2.228 (0.046)	2.776 (0.215)
λ_2^-			0.465 (0.004)		1.040 (0.003)	1.031 (0.041)
ξ_2				3.541 (0.018)	0.113 (0.002)	0.085 (0.000)

Table 5: The overall pricing performance. This table reports the overall pricing errors, defined in Equations (18) and (19), for in-sample and out-of-sample. I use the 2F-CJ model as the benchmark. The error reductions relative to the benchmark (2F-CJ) are in italics below each model. The estimation period is from April 4, 2007 to April 1, 2015, and the out-of-sample period is from April 2, 2015 to December 27, 2017.

	2F	2F-CJ	3FU-CJ	3FZ-ICJ	4F-IJ	4F-ICJ
In-sample	0.1010	0.0761	0.0664	0.0657	0.0638	0.0581
	<i>32.77%</i>		<i>-12.65%</i>	<i>-13.64%</i>	<i>-16.06%</i>	<i>-23.66%</i>
Out-of-sample	0.1143	0.0924	0.0700	0.0787	0.0881	0.0631
	<i>23.78%</i>		<i>-24.23%</i>	<i>-14.73%</i>	<i>-4.59%</i>	<i>-31.64%</i>

Table 6: In-sample Root Mean Square Relative Errors (RMSREs) on the options implied volatilities. Panels A and B report the results of S&P 500 and VIX options, respectively. Moneyness is defined as the strike to future price ratio, $k = K/F(t, T)$. Days-to-maturity (DTM) is in the number of actual days. Panels A.4 and B.4 report the pairwise t -statistics, defined in Equation (23), in a (6×6) matrix. A negative (positive) statistic in entries (i, j) indicates that the model i outperforms (underperforms) the model j . The estimation period is from April 4, 2007 to April 1, 2015. The error reductions relative to the benchmark (2F-CJ) are in italics.

	2F	2F-CJ	3FU-CJ	3FZ-ICJ	4F-IJ	4F-ICJ
Panel A: S&P 500 Options						
Panel A.1: Overall RMSREs						
	0.0928	0.0736	0.0671	0.0681	0.0731	0.0625
	<i>26.10%</i>		<i>-8.73%</i>	<i>-7.38%</i>	<i>-0.65%</i>	<i>-15.07%</i>
Panel A.2: Sorting by moneyness						
$k < 0.8$	0.0899	0.0756	0.0682	0.0777	0.0749	0.0599
$0.85 \leq k < 0.90$	0.0857	0.0628	0.0544	0.0514	0.0669	0.0525
$0.90 \leq k < 0.93$	0.0834	0.0646	0.0539	0.0470	0.0632	0.0493
$0.93 \leq k < 0.95$	0.0783	0.0643	0.0535	0.0475	0.0570	0.0501
$0.95 \leq k < 0.98$	0.0701	0.0635	0.0565	0.0453	0.0520	0.0551
$0.98 \leq k < 1$	0.0961	0.0746	0.0684	0.0433	0.0597	0.0581
$1 \leq k < 1.03$	0.1149	0.0866	0.0819	0.0497	0.0745	0.0580
$1.03 \leq k$	0.1006	0.0791	0.0754	0.0980	0.0922	0.0811
Panel A.3: Sorting by days to maturity						
< 20	0.1196	0.1044	0.0911	0.0652	0.0894	0.0874
20-30	0.0871	0.0645	0.0614	0.0524	0.0704	0.0550
30-50	0.0853	0.0645	0.0628	0.0685	0.0667	0.0575
50-60	0.0852	0.0593	0.0535	0.0581	0.0700	0.0551
60-90	0.0879	0.0657	0.0563	0.0682	0.0679	0.0548
90-180	0.0879	0.0737	0.0691	0.0775	0.0684	0.0602
> 180	0.0944	0.0797	0.0746	0.0912	0.0777	0.0632
Panel A.4: Pairwise t -statistics						
2F	0.00	33.87	36.22	28.18	24.14	37.00
2F-CJ	<i>-33.87</i>	0.00	13.88	9.89	3.45	16.80
3FU-CJ	<i>-36.22</i>	<i>-13.88</i>	0.00	1.65	<i>-6.84</i>	13.18
3FZ-ICJ	<i>-28.18</i>	<i>-9.89</i>	<i>-1.65</i>	0.00	<i>-9.16</i>	7.15
4F-IJ	<i>-24.14</i>	<i>-3.45</i>	6.84	9.16	0.00	21.14
4F-ICJ	<i>-37.00</i>	<i>-16.80</i>	<i>-13.18</i>	<i>-7.15</i>	<i>-21.14</i>	0.00
Panel B: VIX Options						
Panel B.1: Overall RMSREs						
	0.1092	0.0786	0.0657	0.0632	0.0546	0.0537
	<i>39.01%</i>		<i>-16.33%</i>	<i>-19.50%</i>	<i>-30.50%</i>	<i>-31.70%</i>
Panel B.2: Sorting by moneyness						
$k < 0.8$	0.1285	0.1005	0.1250	0.0718	0.0703	0.0738
$0.8 \leq k < 0.9$	0.0961	0.0989	0.0878	0.0837	0.0705	0.0718
$0.9 \leq k < 1.0$	0.1010	0.1058	0.0836	0.0907	0.0698	0.0716
$1.0 \leq k < 1.2$	0.1049	0.0745	0.0557	0.0545	0.0464	0.0452
$1.2 \leq k < 1.4$	0.1082	0.0637	0.0468	0.0555	0.0459	0.0431
$1.4 \leq k < 1.6$	0.1013	0.0656	0.0461	0.0546	0.0480	0.0425
$1.6 \leq k < 1.8$	0.1069	0.0627	0.0457	0.0478	0.0467	0.0437
$1.8 \leq k$	0.1483	0.0619	0.0479	0.0432	0.0518	0.0502
Panel B.3: Sorting by days to maturity						
< 30	0.1397	0.1133	0.1054	0.1019	0.0977	0.0669
30-60	0.1107	0.0792	0.0693	0.0630	0.0469	0.0533
60-90	0.1006	0.0689	0.0504	0.0515	0.0404	0.0446
90-120	0.1001	0.0664	0.0469	0.0452	0.0483	0.0471
> 120	0.0971	0.0646	0.0511	0.0513	0.0544	0.0511
Panel B.4: Pairwise t -statistics						
2F	0.00	14.43	26.33	27.65	32.83	30.73
2F-CJ	<i>-14.43</i>	0.00	14.56	18.24	22.46	20.55
3FU-CJ	<i>-26.33</i>	<i>-14.56</i>	0.00	2.45	2.21	11.25
3FZ-ICJ	<i>-27.65</i>	<i>-18.24</i>	<i>-2.45</i>	0.00	7.17	6.92
4F-IJ	<i>-32.83</i>	<i>-22.46</i>	<i>-2.21</i>	<i>-7.17</i>	0.00	6.16
4F-ICJ	<i>-30.73</i>	<i>-20.55</i>	<i>-11.25</i>	<i>-6.92</i>	<i>-6.16</i>	0.00

Table 7: Out-of-sample Root Mean Square Relative Errors (RMSREs) on the options implied volatilities. Panels A and B report the results of S&P 500 and VIX options, respectively. Moneyness is defined as the strike to future price ratio, $k = K/F(t, T)$. Days-to-maturity (DTM) is in the number of actual days. Panels A.4 and B.4 report the pairwise t -statistics, defined in Equation (23), in a (6×6) matrix. A negative (positive) statistic in entries (i, j) indicates that the model i outperforms (underperforms) the model j . The out-of-sample period is from April 2, 2015 to December 27, 2017. The error reductions relative to the benchmark (2F-CJ) are in italics.

	2F	2F-CJ	3FU-CJ	3FZ-ICJ	4F-IJ	4F-ICJ
Panel A: S&P 500 Options						
Panel A.1: Overall RMSREs						
	0.1146	0.0925	0.0788	0.0738	0.0879	0.0673
	<i>23.90%</i>		<i>-14.81%</i>	<i>-20.18%</i>	<i>-4.98%</i>	<i>-27.25%</i>
Panel A.2: Sorting by moneyness						
$k < 0.8$	0.0633	0.0449	0.0480	0.0595	0.0651	0.0517
$0.85 \leq k < 0.90$	0.0611	0.0482	0.0490	0.0484	0.0757	0.0547
$0.90 \leq k < 0.93$	0.0589	0.0556	0.0444	0.0533	0.0743	0.0449
$0.93 \leq k < 0.95$	0.0532	0.0600	0.0406	0.0598	0.0720	0.0413
$0.95 \leq k < 0.98$	0.0511	0.0606	0.0430	0.0553	0.0711	0.0489
$0.98 \leq k < 1$	0.1034	0.0723	0.0582	0.0520	0.0723	0.0578
$1 \leq k < 1.03$	0.1733	0.1380	0.1101	0.0682	0.0977	0.0821
$1.03 \leq k$	0.1898	0.1494	0.1357	0.1318	0.1342	0.1068
Panel A.3: Sorting by days to maturity						
< 20	0.1430	0.1248	0.0939	0.0745	0.0992	0.0816
20-30	0.1155	0.0923	0.0779	0.0618	0.0901	0.0687
30-50	0.1014	0.0817	0.0746	0.0780	0.0862	0.0637
50-60	0.1102	0.0849	0.0735	0.0614	0.0830	0.0629
60-90	0.1077	0.0850	0.0735	0.0654	0.0805	0.0598
90-180	0.0950	0.0759	0.0753	0.0925	0.0824	0.0599
> 180	0.1109	0.0785	0.0819	0.1212	0.0909	0.0682
Panel A.4: Pairwise t -statistics						
2F	0.00	31.96	36.25	27.28	16.32	34.71
2F-CJ	<i>-31.96</i>	0.00	13.74	11.00	2.58	16.46
3FU-CJ	<i>-36.25</i>	<i>-13.74</i>	0.00	<i>-0.31</i>	<i>-6.03</i>	15.20
3FZ-ICJ	<i>-27.28</i>	<i>-11.00</i>	0.31	0.00	<i>-6.63</i>	12.12
4F-IJ	<i>-16.32</i>	<i>-2.58</i>	6.03	6.63	0.00	14.87
4F-ICJ	<i>-34.71</i>	<i>-16.46</i>	<i>-15.20</i>	<i>-12.12</i>	<i>-14.87</i>	0.00
Panel B: VIX Options						
Panel B.1: Overall RMSREs						
	0.1140	0.0922	0.0612	0.0837	0.0883	0.0590
	<i>23.66%</i>		<i>-33.67%</i>	<i>-9.27%</i>	<i>-4.20%</i>	<i>-36.04%</i>
Panel B.2: Sorting by moneyness						
$k < 0.8$	0.1797	0.0832	0.0905	0.0799	0.0887	0.0987
$0.8 \leq k < 0.9$	0.1193	0.1251	0.0849	0.1289	0.1086	0.0875
$0.9 \leq k < 1.0$	0.1183	0.1216	0.0826	0.1261	0.1059	0.0843
$1.0 \leq k < 1.2$	0.1231	0.0917	0.0714	0.0843	0.0884	0.0663
$1.2 \leq k < 1.4$	0.1006	0.0750	0.0517	0.0706	0.0861	0.0495
$1.4 \leq k < 1.6$	0.0851	0.0857	0.0438	0.0682	0.0889	0.0370
$1.6 \leq k < 1.8$	0.0857	0.0884	0.0395	0.0627	0.0746	0.0342
$1.8 \leq k$	0.1341	0.0805	0.0422	0.0592	0.0744	0.0370
Panel B.3: Sorting by days to maturity						
< 30	0.1518	0.1266	0.0977	0.1324	0.1091	0.0884
30-60	0.0825	0.0836	0.0469	0.0793	0.0791	0.0496
60-90	0.0855	0.0780	0.0404	0.0713	0.0804	0.0455
90-120	0.1077	0.0801	0.0483	0.0587	0.0768	0.0469
> 120	0.1298	0.0830	0.0544	0.0476	0.0936	0.0533
Panel B.4: Pairwise t -statistics						
2F	0.00	8.87	26.36	16.36	13.71	21.28
2F-CJ	<i>-8.87</i>	0.00	20.56	8.91	5.53	16.90
3FU-CJ	<i>-26.36</i>	<i>-20.56</i>	0.00	<i>-20.44</i>	<i>-6.46</i>	1.53
3FZ-ICJ	<i>-16.36</i>	<i>-8.91</i>	20.44	0.00	2.70	20.26
4F-IJ	<i>-13.71</i>	<i>-5.53</i>	6.46	<i>-2.70</i>	0.00	7.23
4F-ICJ	<i>-21.28</i>	<i>-16.90</i>	<i>-1.53</i>	<i>-20.26</i>	<i>-7.23</i>	0.00

Table 8: Fit to option characteristics. This table reports the root-mean-square errors from fitting the implied volatility surface characteristics. IV skew is defined as the difference between the IVs of deep out-of-the-money (OTM) call and OTM put options. Specifically, VIX skew equals deep OTM call IV minus deep OTM put IV, whereas SPX skew equals deep OTM put IV minus deep OTM call IV. For S&P 500 options, short-term (long-term) options are those with days to maturity < 45 (> 270) days, and deep OTM call (put) options have moneyness, $K/F, > 1.03$ (< 0.9). For VIX options, short-term (long-term) options are those with days to maturity < 45 (> 120) days, and deep OTM call (put) options have moneyness > 1.8 (< 0.8). ATM options have moneyness close to 1 for both types of options. The error reductions relative to the benchmark (2F-CJ) are in italics below each model. The estimation period is from April 4, 2007 to April 1, 2015, and the out-of-sample period is from April 2, 2015, to December 27, 2017.

	2F	2F-CJ	3FU-CJ	3FZ-ICJ	4F-IJ	4F-ICJ
Panel A: S&P 500 options						
Short-term ATM IV	0.0090 <i>8.43%</i>	0.0083	0.0118 <i>42.17%</i>	0.0083 <i>0.00%</i>	0.0189 <i>127.71%</i>	0.0091 <i>9.64%</i>
Long-term ATM IV	0.0167 <i>9.15%</i>	0.0153	0.0104 <i>-32.03%</i>	0.0083 <i>-45.75%</i>	0.0083 <i>-45.75%</i>	0.0071 <i>-53.59%</i>
Short-term skew	0.0421 <i>8.79%</i>	0.0387	0.0357 <i>-7.75%</i>	0.0320 <i>-17.31%</i>	0.0374 <i>-3.36%</i>	0.0313 <i>-19.12%</i>
Long-term skew	0.0408 <i>9.68%</i>	0.0372	0.0340 <i>-8.60%</i>	0.0355 <i>-4.57%</i>	0.0385 <i>3.49%</i>	0.0293 <i>-21.24%</i>
Panel B: VIX options						
Short-term ATM IV	0.1044 <i>6.21%</i>	0.0983	0.0933 <i>-5.09%</i>	0.0868 <i>-11.70%</i>	0.0561 <i>-42.93%</i>	0.0634 <i>-35.50%</i>
Long-term ATM IV	0.0609 <i>22.78%</i>	0.0496	0.0331 <i>-33.27%</i>	0.0329 <i>-33.67%</i>	0.0371 <i>-25.20%</i>	0.0343 <i>-30.85%</i>
Short-term skew	0.1840 <i>-1.55%</i>	0.1869	0.1325 <i>-29.11%</i>	0.1474 <i>-21.13%</i>	0.1286 <i>-31.19%</i>	0.0996 <i>-46.71%</i>
Long-term skew	0.0823 <i>28.79%</i>	0.0639	0.0528 <i>-17.37%</i>	0.0558 <i>-12.68%</i>	0.0638 <i>-0.16%</i>	0.0558 <i>-12.68%</i>

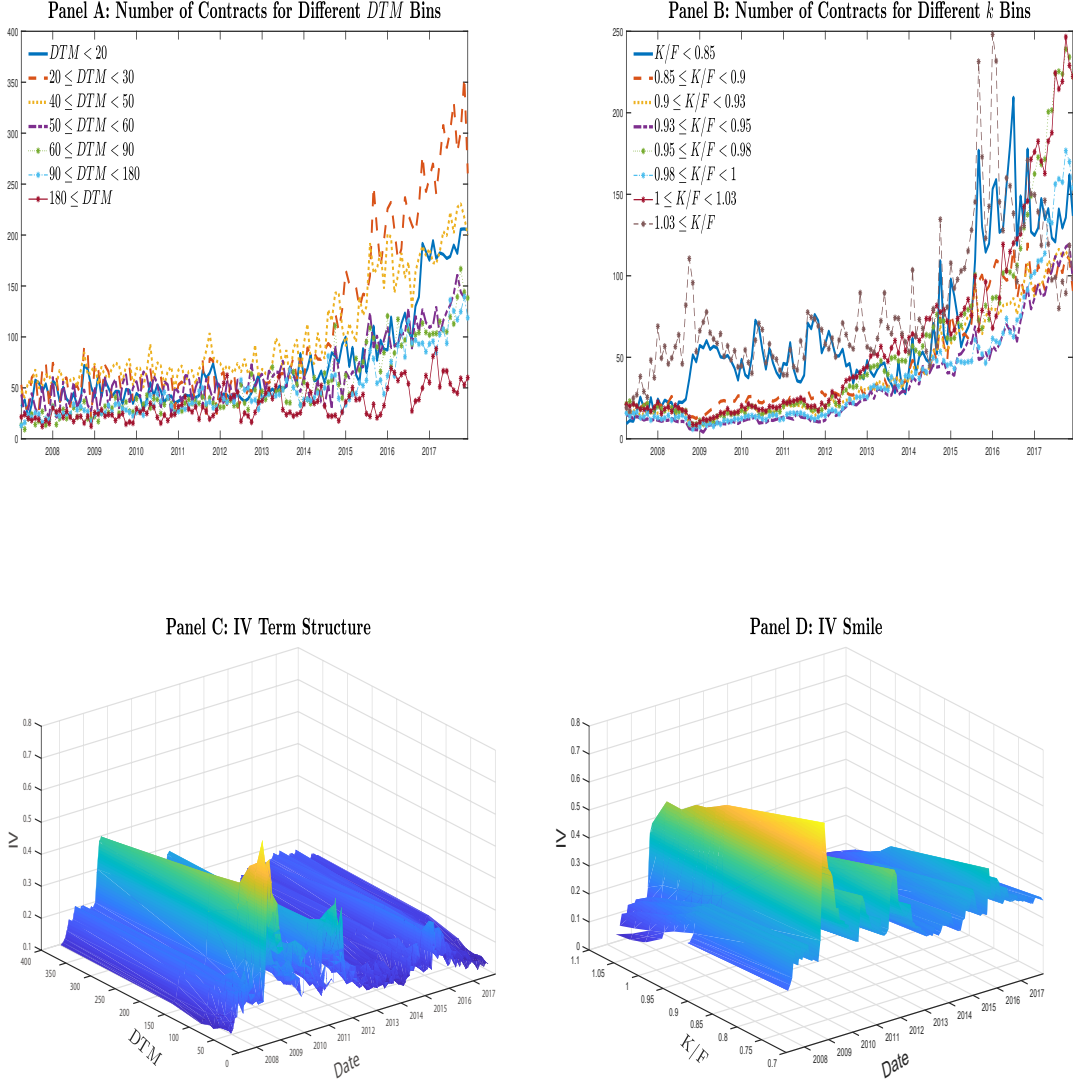


Fig. 1. This figure shows the time-series plots of S&P 500 options data from April 4, 2007, to December 27, 2017, in monthly frequency. Panels A and B plot the number of contracts for different days-to-maturity and moneyness bins, respectively. Panels C and D display VIX implied volatility (IV) slope along with the term structure and the moneyness dimension, respectively. Moneyness is defined as the strike to future price ratio, K/F . Days-to-maturity (DTM) is in the number of actual days. The implied volatilities are calculated using the Black-Scholes formula.

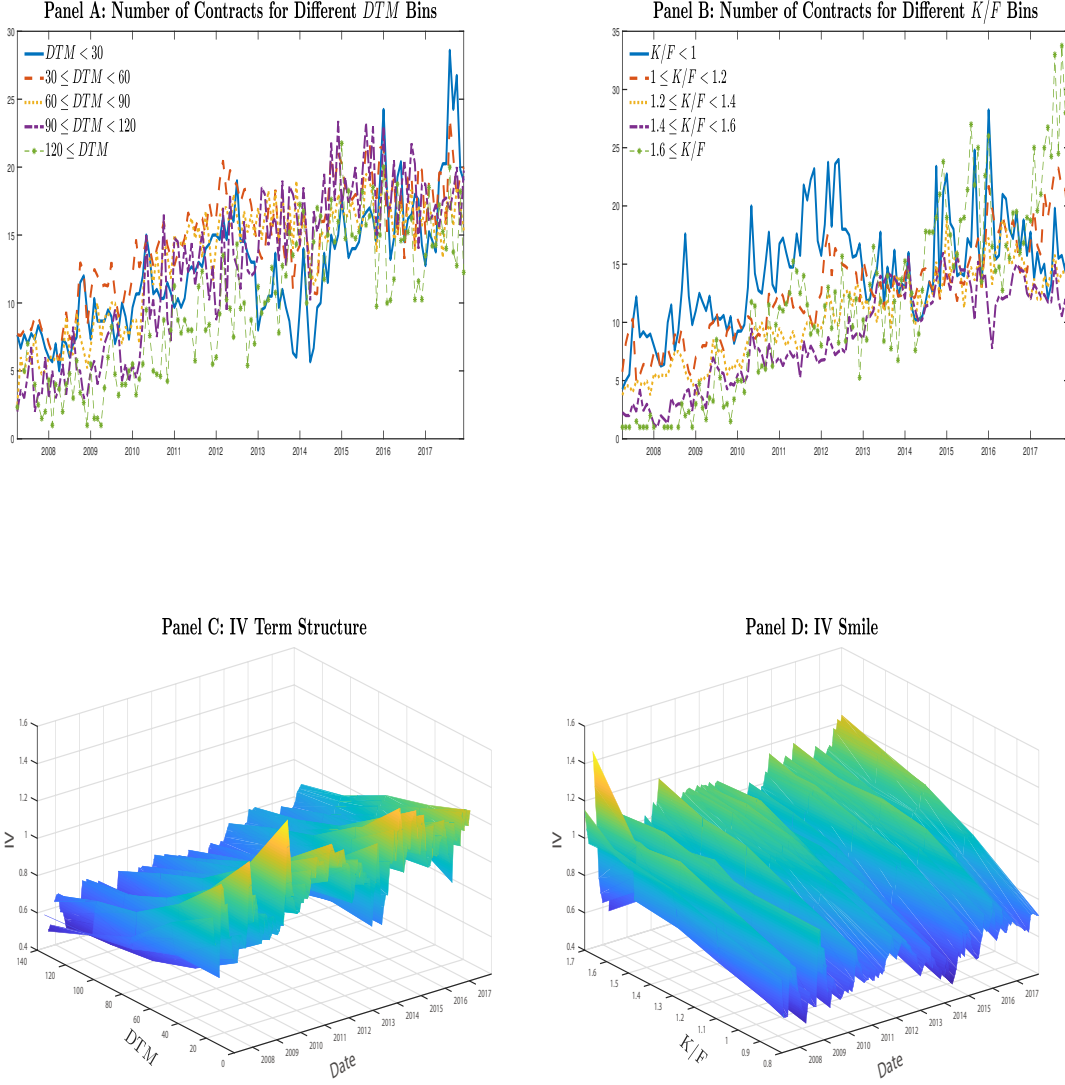


Fig. 2. This figure shows the time-series plots of VIX options data from April 4, 2007, to December 27, 2017, in monthly frequency. Panels A and B plot the number of contracts for different days-to-maturity and moneyness bins, respectively. Panels C and D display VIX implied volatility (IV) slope along with the term structure and the moneyness dimension, respectively. Moneyness is defined as the strike to future price ratio, K/F . Days-to-maturity (DTM) is in the number of actual days. The implied volatilities are calculated using the Black-Scholes formula.

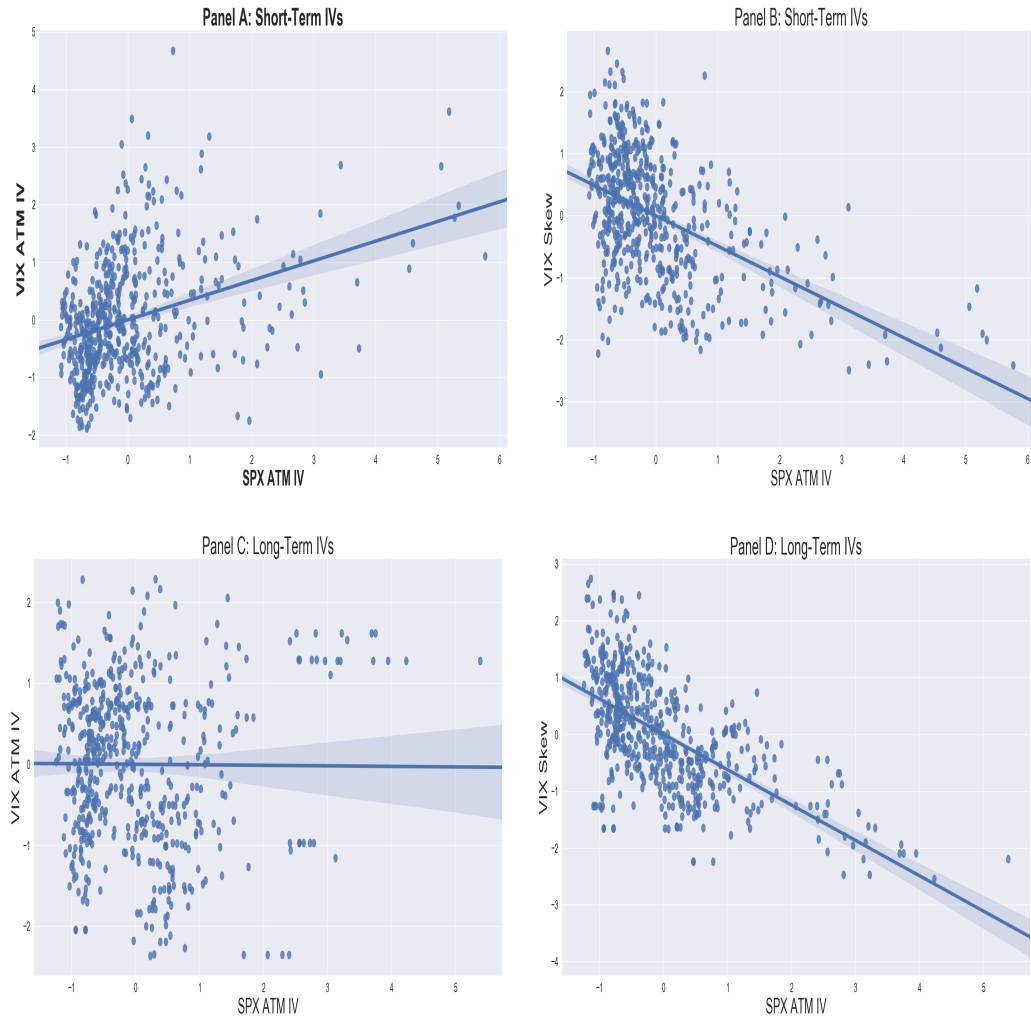


Fig. 3. This figure shows scatter plots of the S&P 500 at-the-money implied volatility (SPX ATM IV) against VIX IV characteristics. IV skew is defined as the difference between the IVs of deep out-of-the-money (OTM) call and OTM put options. Specifically, VIX skew equals deep OTM call IV minus deep OTM put IV, whereas SPX skew equals deep OTM put IV minus deep OTM call IV. For S&P 500 options, short-term (long-term) options are those with days to maturity < 45 (> 270) days, and deep OTM call (put) options have moneyness, K/F , > 1.03 (< 0.9). For VIX options, short-term (long-term) options are those with days to maturity < 45 (> 120) days, and deep OTM call (put) options have moneyness > 1.8 (< 0.8). ATM options have moneyness close to 1 for both types of options.

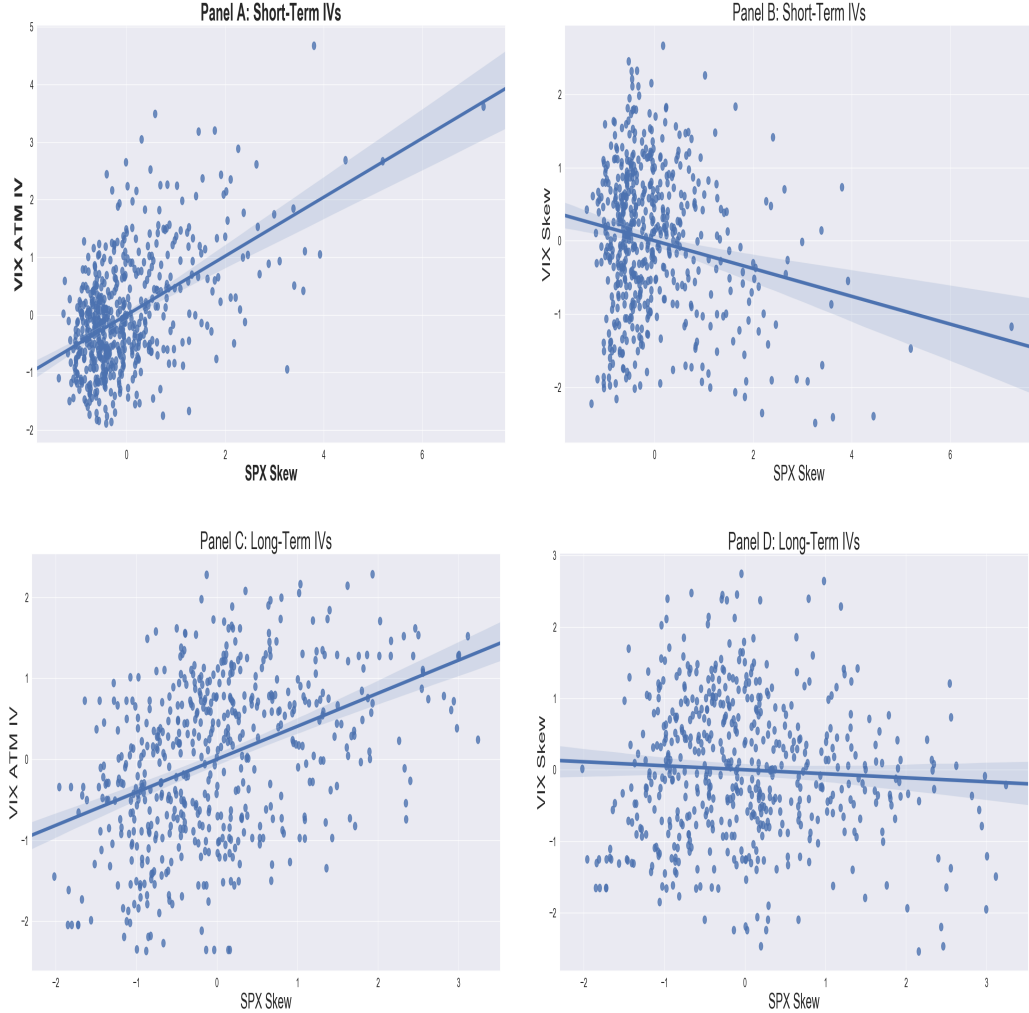


Fig. 4. This figure shows scatter plots of the S&P 500 skew (SPX skew) against VIX IV characteristics. IV skew is defined as the difference between the IVs of deep out-of-the-money (OTM) call and OTM put options. Specifically, VIX skew equals deep OTM call IV minus deep OTM put IV, whereas SPX skew equals deep OTM put IV minus deep OTM call IV. For S&P 500 options, short-term (long-term) options are those with days to maturity < 45 (> 270) days, and deep OTM call (put) options have moneyness, K/F , > 1.03 (< 0.9). For VIX options, short-term (long-term) options are those with days to maturity < 45 (> 120) days, and deep OTM call (put) options have moneyness > 1.8 (< 0.8). ATM options have moneyness close to 1 for both types of options

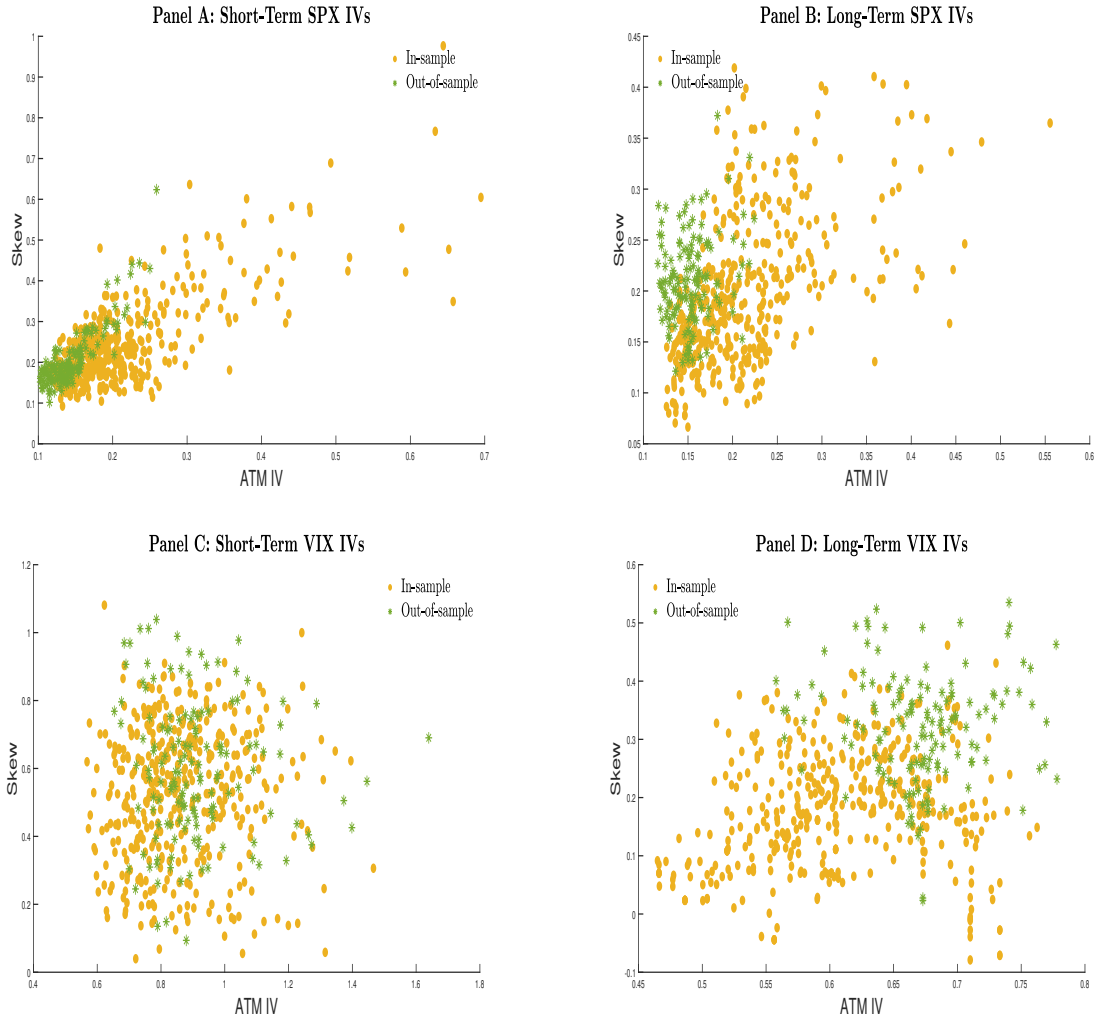


Fig. 5. This figure shows scatter plots of IV skew against ATM IV during in- and out-of sample. IV skew is defined as the difference between the IVs of deep out-of-the-money (OTM) call and OTM put options. Specifically, VIX skew equals deep OTM call IV minus deep OTM put IV, whereas SPX skew equals deep OTM put IV minus deep OTM call IV. For S&P 500 options, short-term (long-term) options are those with days to maturity < 45 (> 270) days, and deep OTM call (put) options have moneyness, K/F , > 1.03 (< 0.9). For VIX options, short-term (long-term) options are those with days to maturity < 45 (> 120) days, and deep OTM call (put) options have moneyness > 1.8 (< 0.8). ATM options have moneyness close to 1 for both types of options. The in-sample period is from April 4, 2007, to April 1, 2015, and the out-of-sample period is from April 2, 2015, to December 27, 2017.

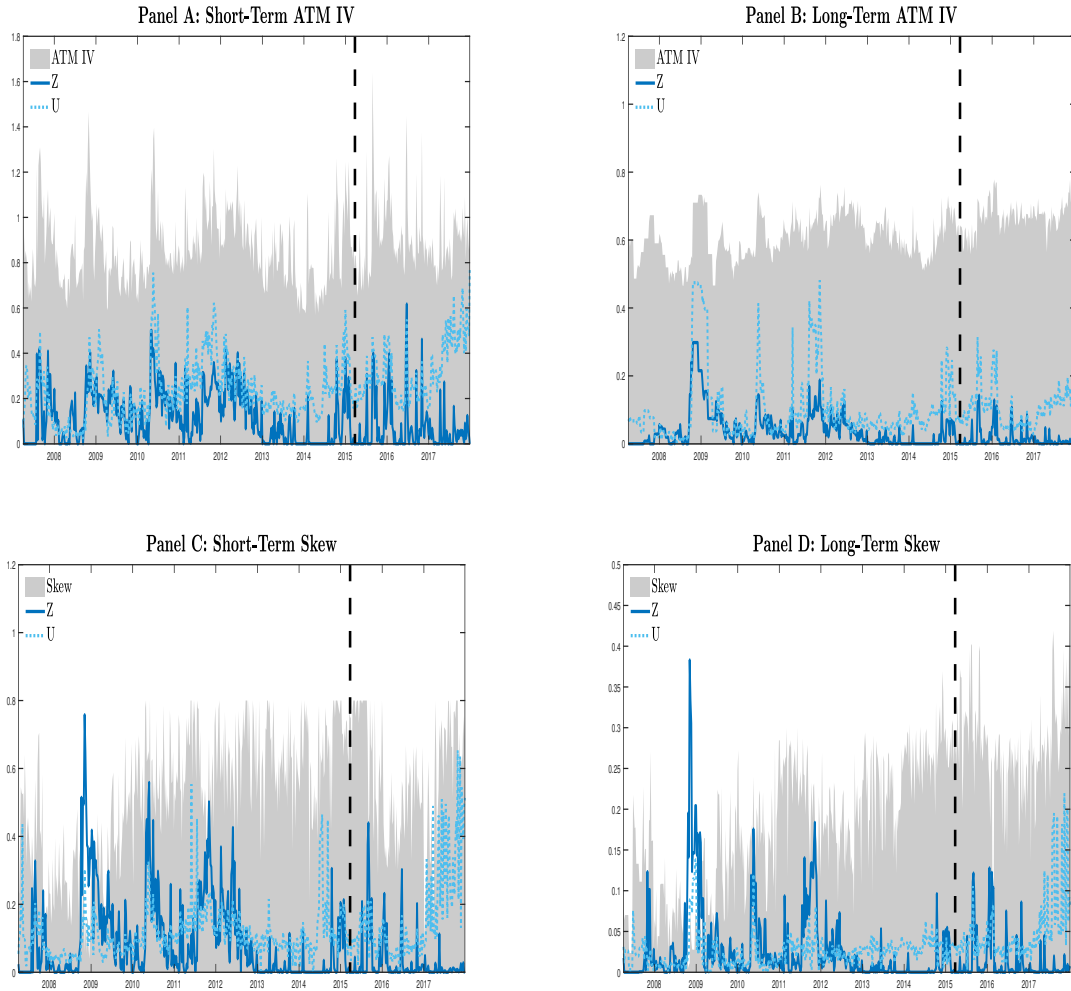


Fig. 6. This figure shows the effects of Z and U on the VIX options characteristics. The effect of either risk factor is measured via the change of the characteristics stemming from increases and decreases in factor by 50% relative to the current estimate value. The solid (dotted) lines correspond to the effect of Z (U), and the shaded area indicates the IV characteristics (ATM IV and skew). The vertical dotted line in each panel splits the full sample into in-sample and out-of-sample periods. IV skew is defined as the difference between the IVs of deep out-of-the-money (OTM) call and OTM put options. Specifically, VIX skew equals deep OTM call IV minus deep OTM put IV, whereas SPX skew equals deep OTM put IV minus deep OTM call IV. For S&P 500 options, short-term (long-term) options are those with days to maturity < 45 (> 270) days, and deep OTM call (put) options have moneyness, K/F , > 1.03 (< 0.9). For VIX options, short-term (long-term) options are those with days to maturity < 45 (> 120) days, and deep OTM call (put) options have moneyness > 1.8 (< 0.8). ATM options have moneyness close to 1 for both types of options. The in-sample period is from April 4, 2007, to April 1, 2015, and the out-of-sample period is from April 2, 2015, to December 27, 2017.

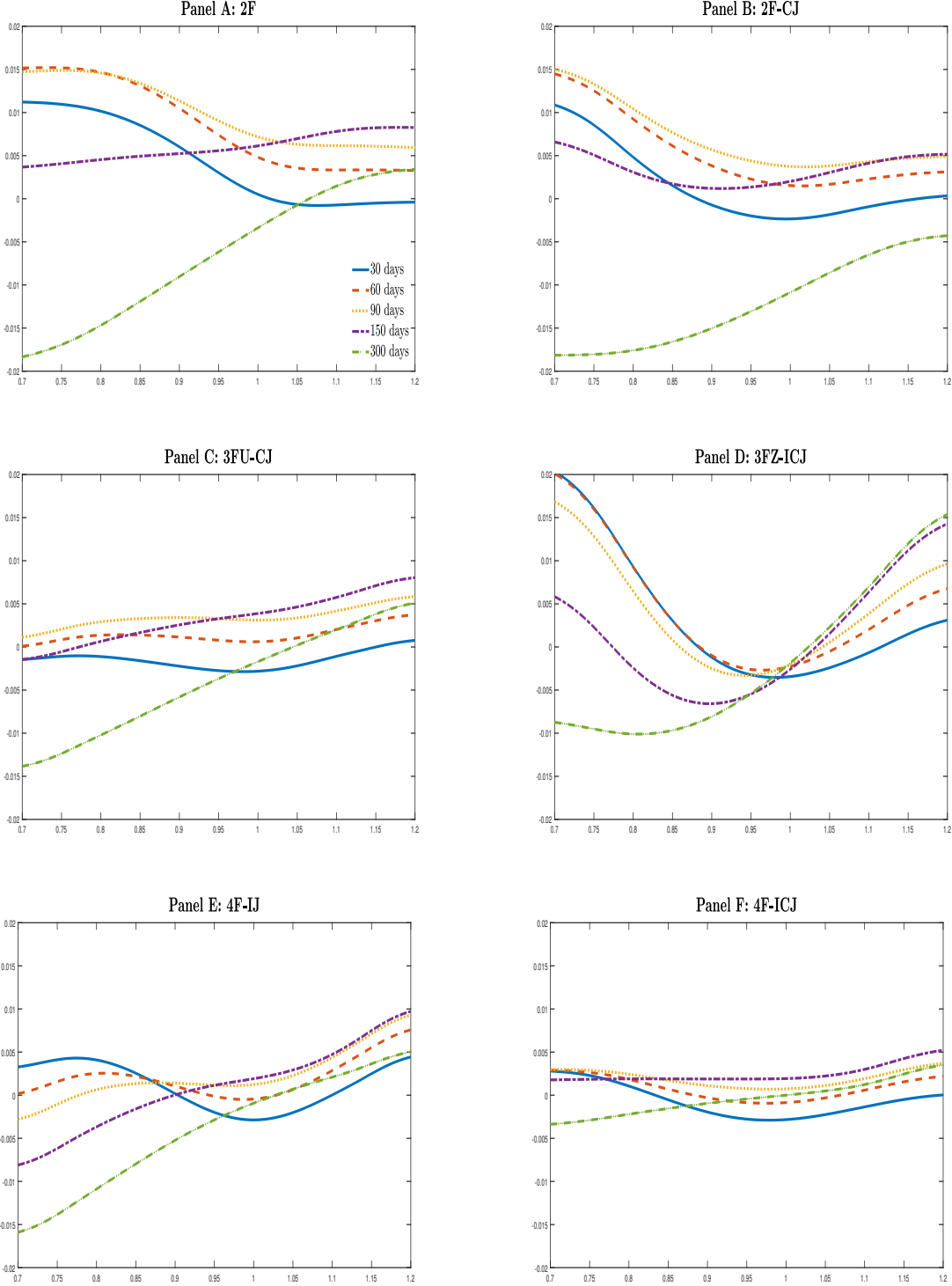


Fig. 7. This figure shows smoothed mean pricing errors of S&P 500 options. The pricing errors are defined as the difference between the model-implied implied volatility (IV) and the market-observed IV. Using independent Gaussian kernels, I estimate the mean pricing errors at fixed moneyness and maturities. Each panel denotes one model. The different lines in each panel denote different maturities, as shown in Panel A.

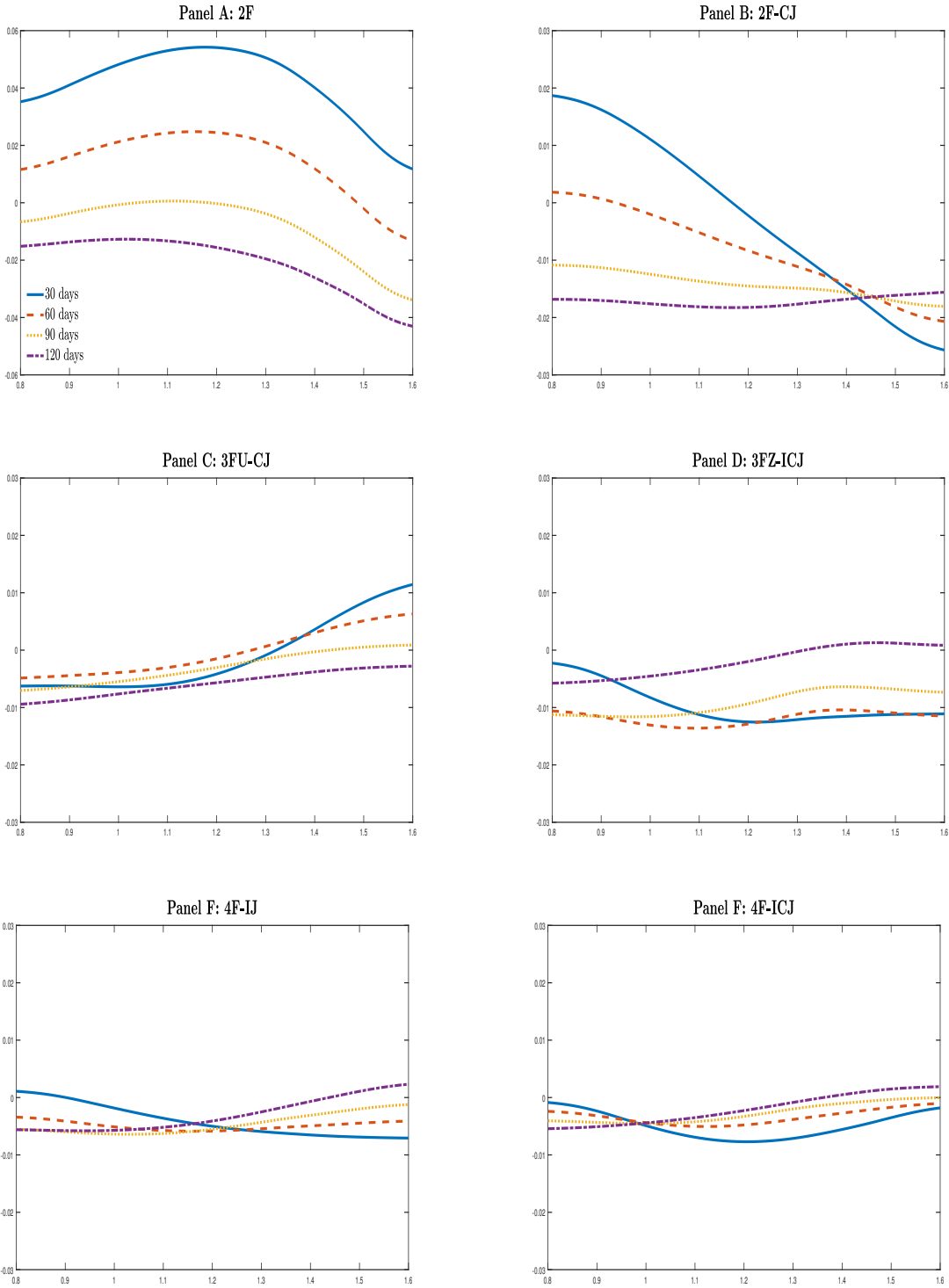


Fig. 8. This figure shows smoothed mean pricing errors of VIX options. The pricing errors are defined as the difference between the model-implied implied volatility (IV) and the market-observed IV. Using independent Gaussian kernels, I estimate the mean pricing errors at fixed moneyness and maturities. Each panel denotes one model. The different lines in each panel denote different maturities, as shown in Panel A.

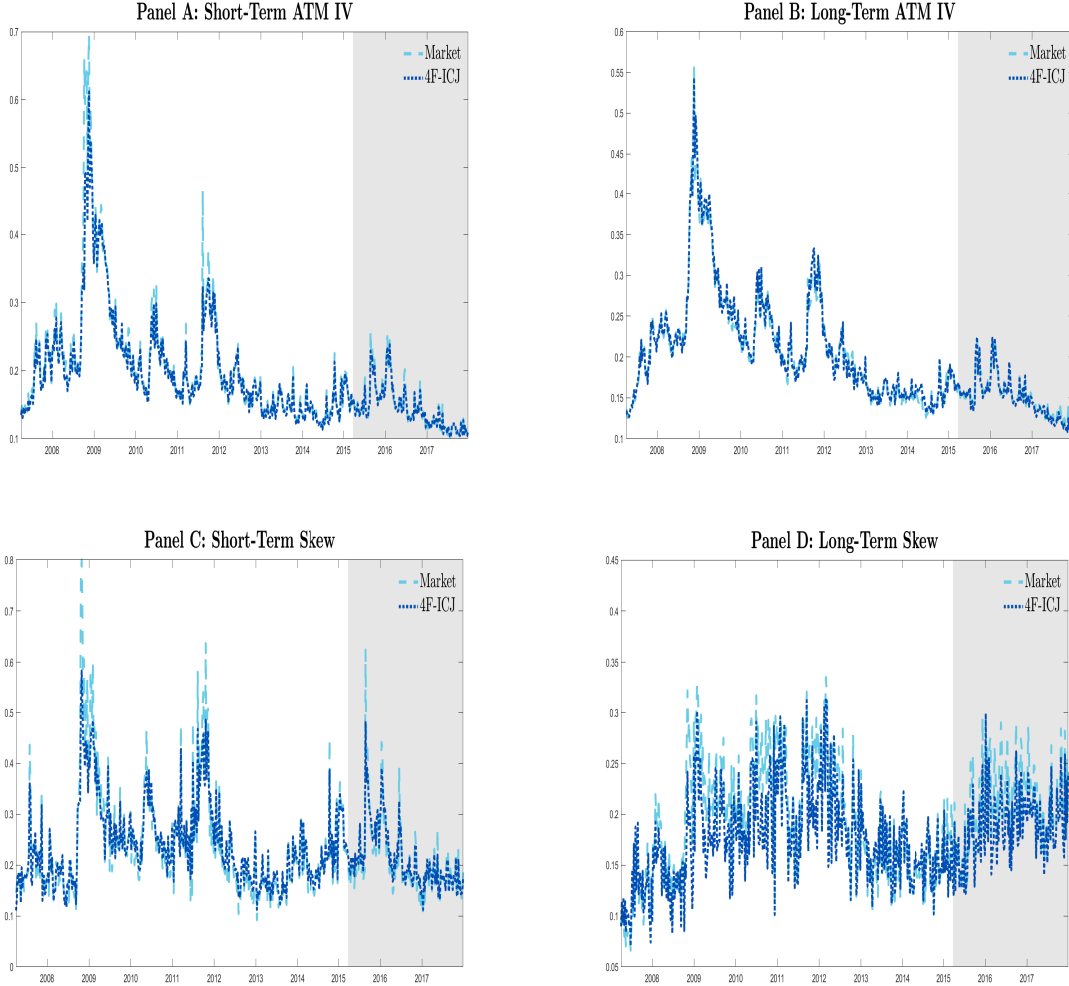


Fig. 9. This figure shows the model-implied fit to the S&P 500 option characteristics. The dashed lines correspond to the market observed characteristics, and the dotted lines refer to the fit by the 4F-ICJ model. The shaded part of the graph represents the out-of-sample period. IV skew is defined as the difference between the IVs of deep out-of-the-money (OTM) call and OTM put options. Specifically, VIX skew equals deep OTM call IV minus deep OTM put IV, whereas SPX skew equals deep OTM put IV minus deep OTM call IV. For S&P 500 options, short-term (long-term) options are those with days to maturity < 45 (> 270) days, and deep OTM call (put) options have moneyness, K/F , > 1.03 (< 0.9). For VIX options, short-term (long-term) options are those with days to maturity < 45 (> 120) days, and deep OTM call (put) options have moneyness > 1.8 (< 0.8). ATM options have moneyness close to 1 for both types of options. The in-sample period is from April 4, 2007, to April 1, 2015, and the out-of-sample period is from April 2, 2015, to December 27, 2017.

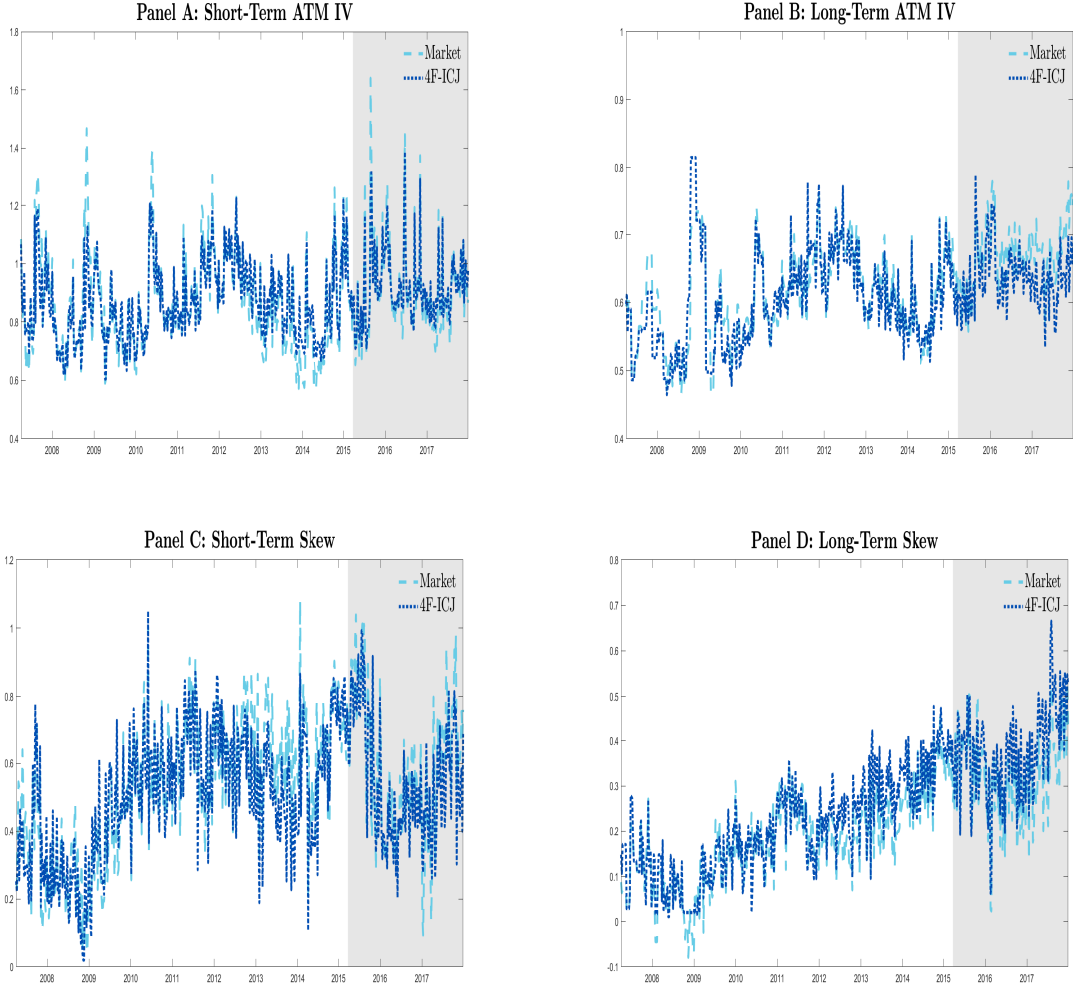


Fig. 10. This figure shows the model-implied fit to the VIX option characteristics. The dashed lines correspond to the market observed characteristics, and the dotted lines refer to the fit by the 4F-ICJ model. The shaded part of the graph represents the out-of-sample period. IV skew is defined as the difference between the IVs of deep out-of-the-money (OTM) call and OTM put options. Specifically, VIX skew equals deep OTM call IV minus deep OTM put IV, whereas SPX skew equals deep OTM put IV minus deep OTM call IV. For S&P 500 options, short-term (long-term) options are those with days to maturity < 45 (> 270) days, and deep OTM call (put) options have moneyness, K/F , > 1.03 (< 0.9). For VIX options, short-term (long-term) options are those with days to maturity < 45 (> 120) days, and deep OTM call (put) options have moneyness > 1.8 (< 0.8). ATM options have moneyness close to 1 for both types of options. The in-sample period is from April 4, 2007, to April 1, 2015, and the out-of-sample period is from April 2, 2015, to December 27, 2017.

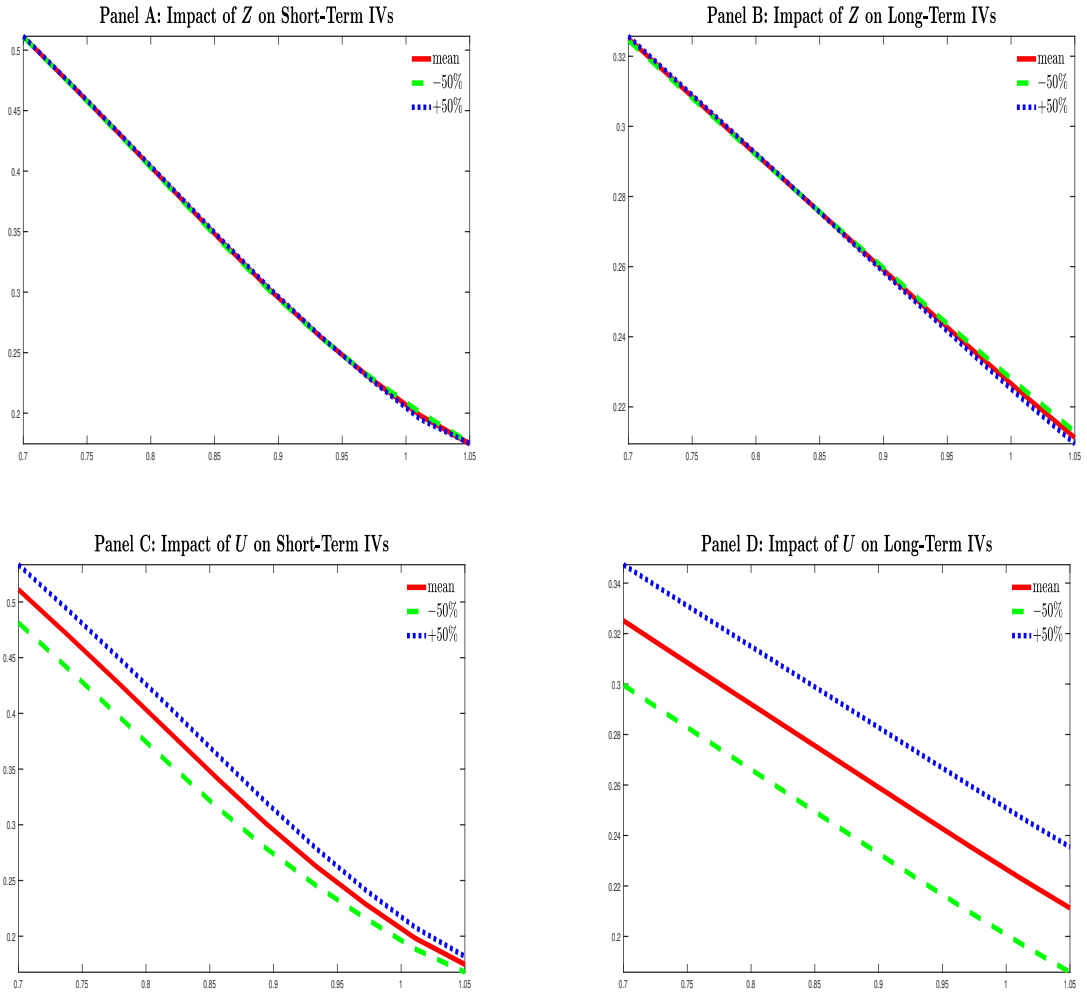


Fig. 11. This figure illustrates the impacts of Z and U on S&P 500 implied volatility smirk. The simulated IV smirk is calculated based on the 4F-ICJ model with parameter estimates in Table 4. The solid lines are the mean value of IVs computed by using the mean levels of the risk factors. Dotted (dashed) lines are computed by increasing (decreasing) the corresponding factor by 50% and fixing other risk factors.

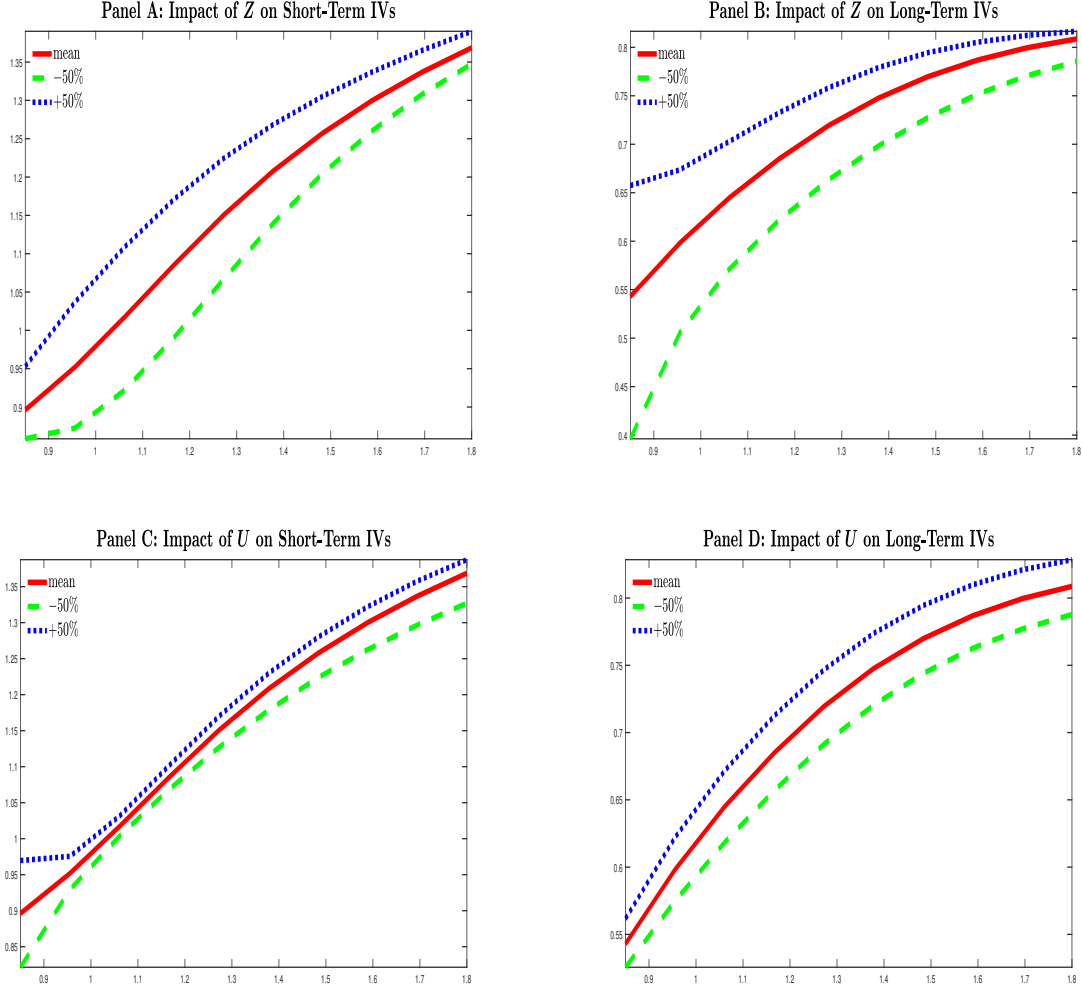


Fig. 12. This figure illustrates the impacts of Z and U on VIX implied volatility smirk. The simulated IV smirk is calculated based on the 4F-ICJ model with parameter estimates in Table 4. The solid lines are the mean value of IVs computed by using the mean levels of the risk factors. Dotted (dashed) lines are computed by increasing (decreasing) the corresponding factor by 50% and fixing other risk factors.

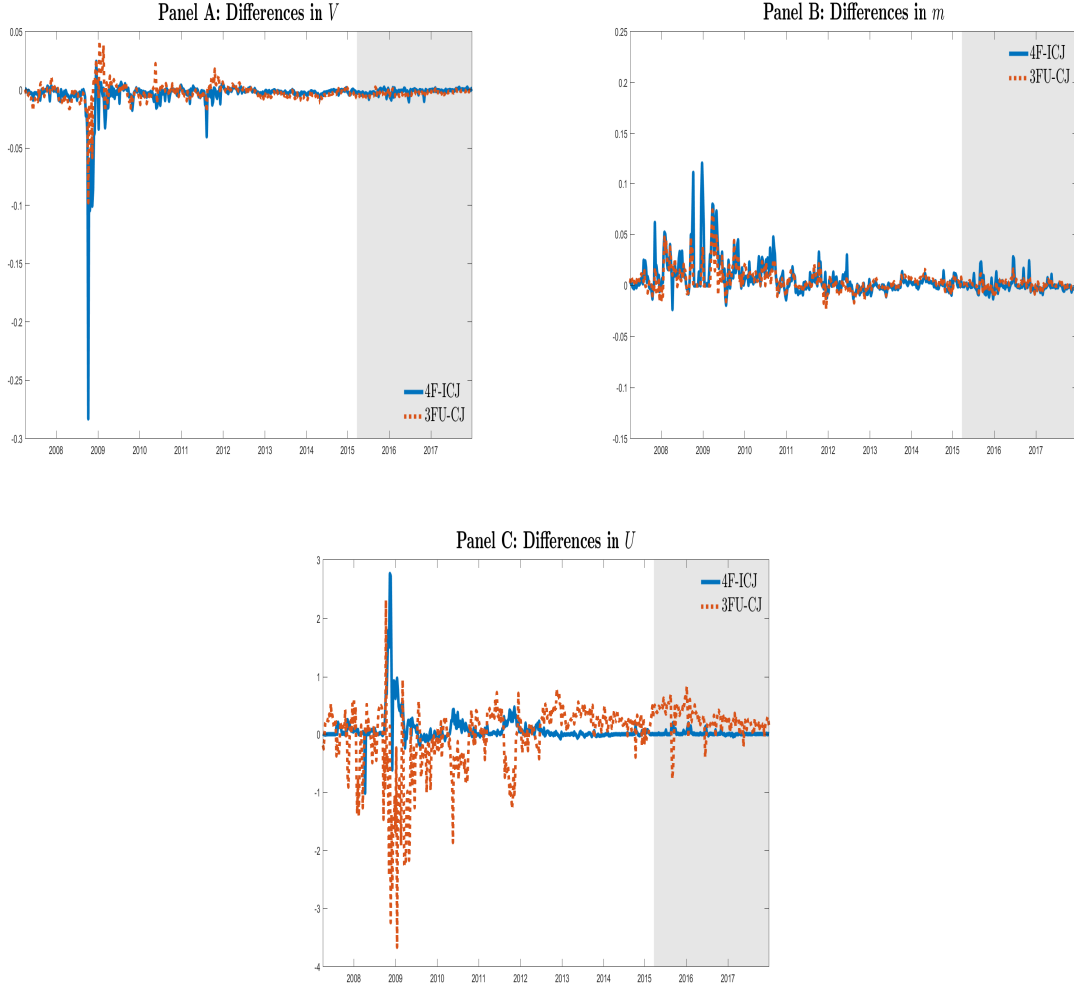


Fig. 13. This figure shows the difference between the filtered state processes of the 4F-ICJ and 3FU-CJ models for 1) using both S&P 500 and VIX options and 2) using S&P 500 options only. The solid lines correspond to the result from the 4F-ICJ model, and dotted lines refer to the result from the 3FU-CJ model. The shaded part of the graph represents the out-of-sample period. The in-sample period is from April 4, 2007, to April 1, 2015, and the out-of-sample period is from April 2, 2015, to December 27, 2017.

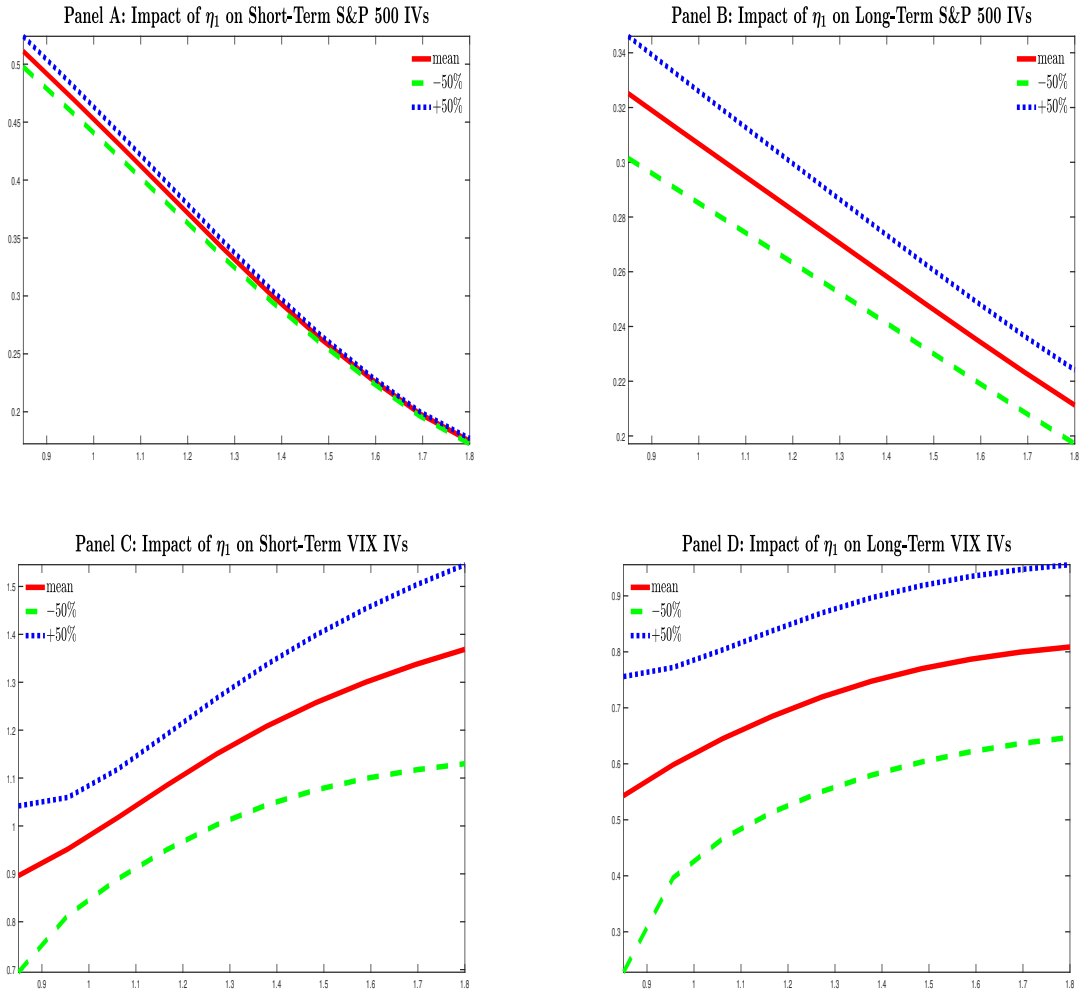


Fig. 14. This figure illustrates the impacts of η_1 on options implied volatility smirk. The simulated IV smirk is calculated based on the 4F-ICJ model with parameter estimates in Table 4. The solid lines are IVs computed by using the estimated value of η_1 . Dotted (dashed) lines are computed by increasing (decreasing) η_1 by 50% and fixing parameters.

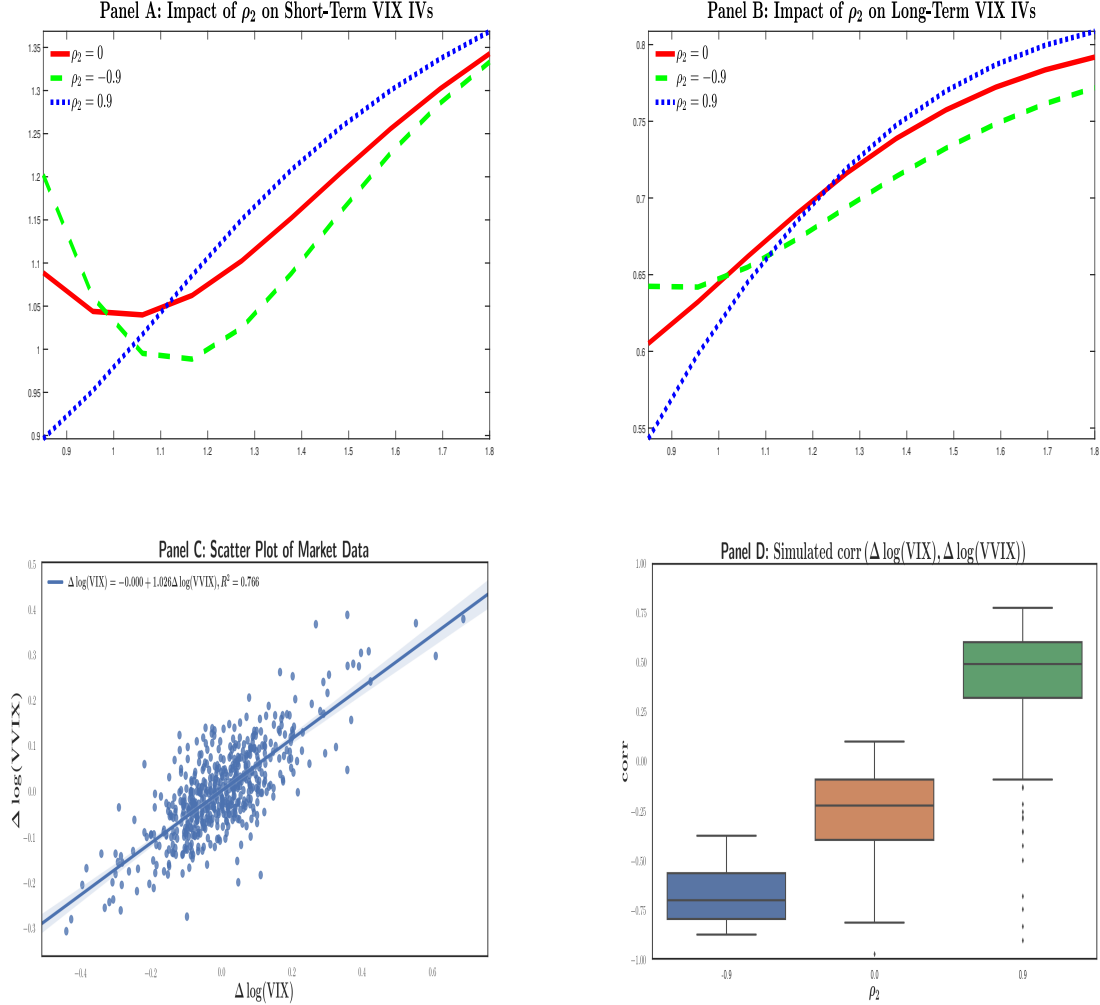


Fig. 15. This figure illustrates the impacts of ρ_2 on VIX options implied volatility smirk. In Panels A and B, the simulated IV smirk is calculated based on the 4F-ICJ model with parameter estimates in Table 4. The solid lines are IVs computed by setting ρ_2 at 0. Dotted (dashed) lines are computed by setting ρ_2 at 0.9 (-0.9). Panel C shows the scatter plot of market VVIX log returns against VIX log returns. Panel D displays the result from the Monte Carlo simulation. Specifically, I simulate the dynamics of states based on Equations (1) - (5) for 500 days. For each day, I generate a range of 30-day VIX options with fixed strikes ($0.8 \leq K/F \leq 1.2$) based on the simulated states and estimated parameters of the 4F-ICJ model in Table 4. Next, I calculate the VIX index based on Equation (11) and VVIX index based on Equation (24). Finally, I calculate the correlation between VIX log-returns and VVIX log-returns, denoted by corr . To get the distribution of simulated correlation, I repeat the simulation for 1000 times.